Chapter 5

Brief history of climate: causes and mechanisms

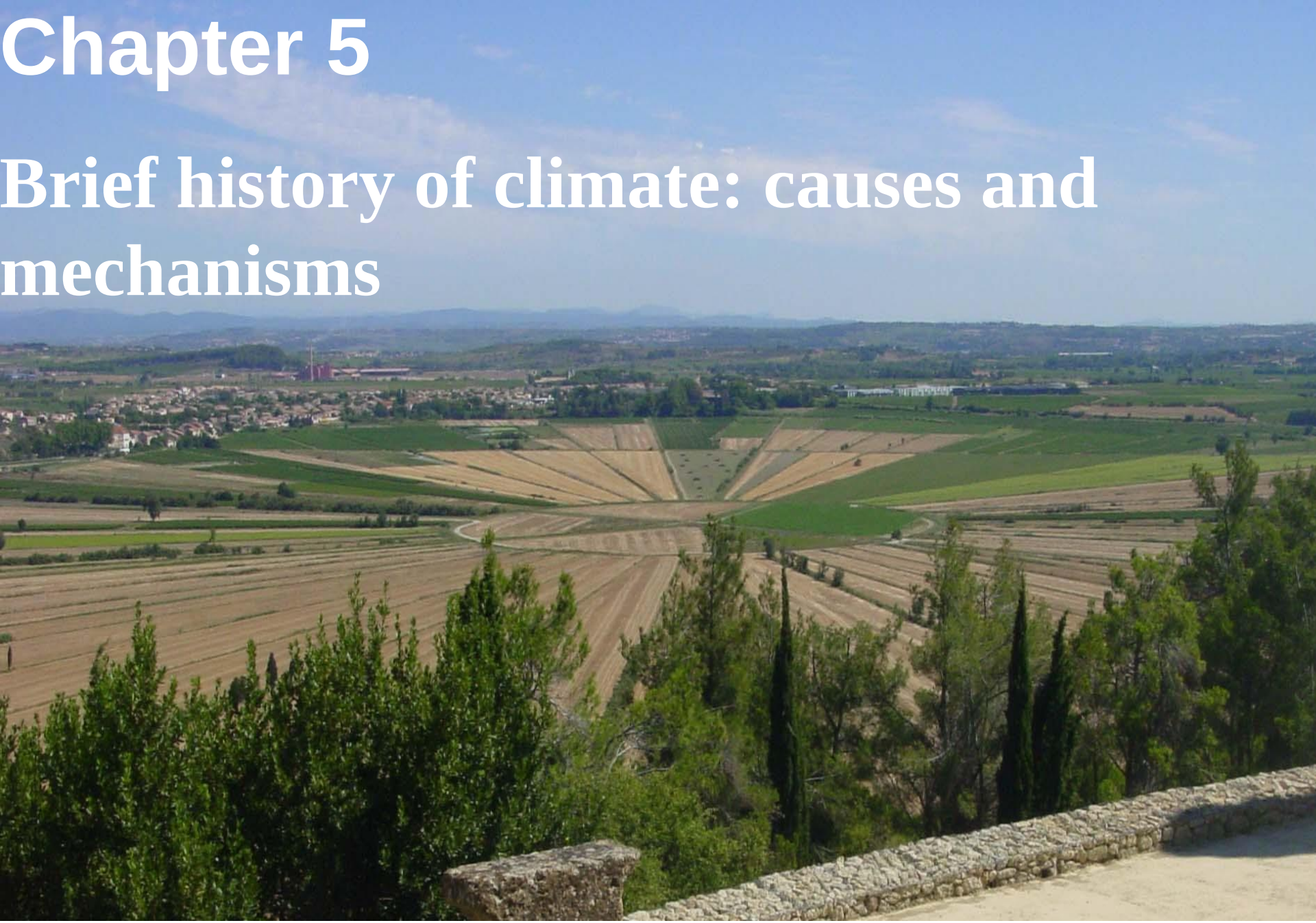

Outline

Investigation of the role of the external forcing and of the internal dynamics.

Analysis of key periods to illustrate dominant processes.

Forced and internal variability

Forced variability: driven by changes in external forcing

Internal variability: caused by interactions between various elements of the system

Forced and internal variability

Forced variability: possible to find the *ultimate cause* of the observed changes

Internal variability: only the chain of events can be identified, the *proximate cause*.

Forced and internal variability

The climate system is sensitive to small perturbations.

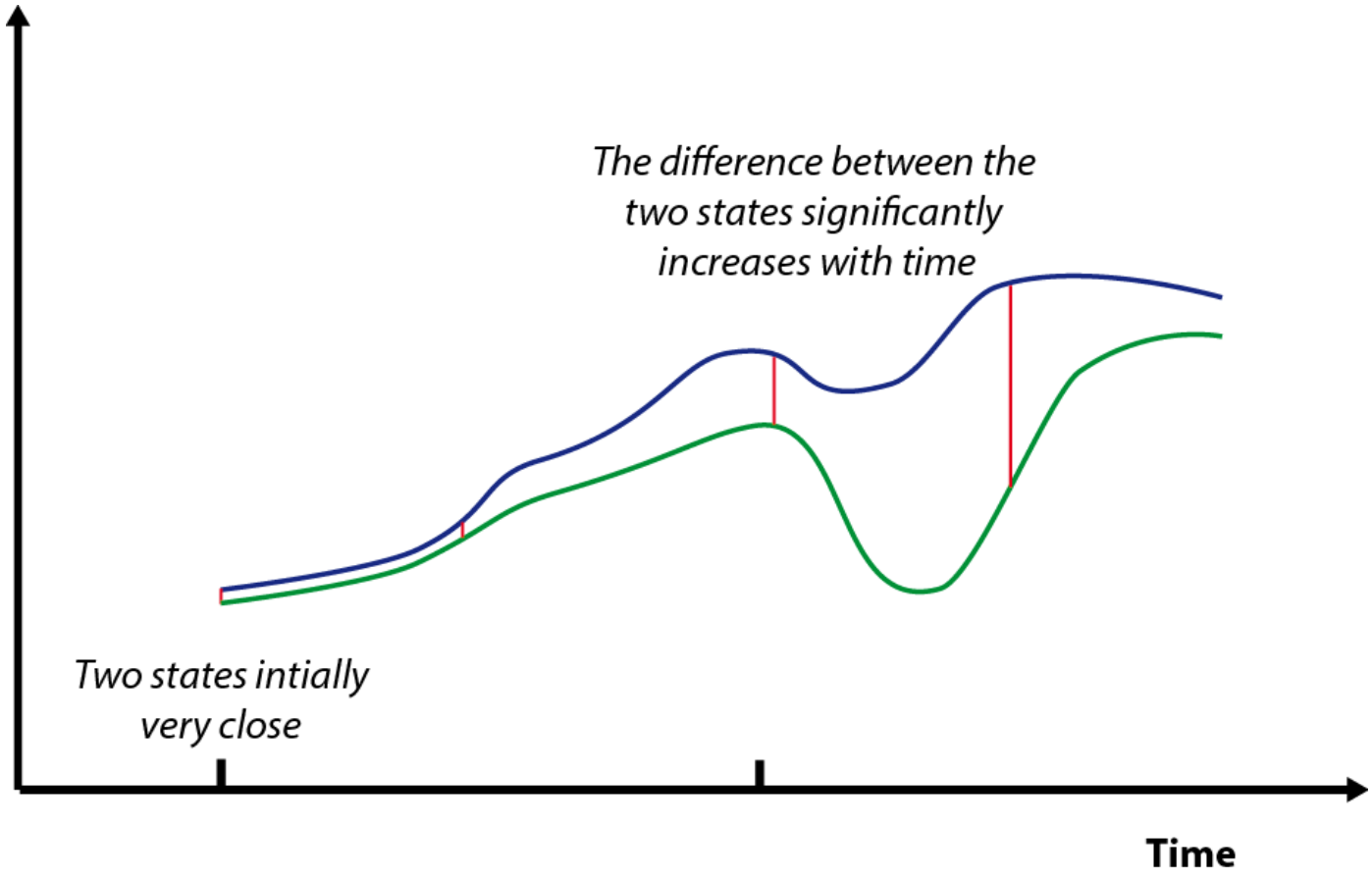

Forced and internal variability

The climate system is sensitive to small perturbations.

Consequences:

1. The skill of weather forecasts is limited in time.
2. Two simulations include different realisations of internal variability.
3. An agreement between simulations and observations on the timing of unforced events is not expected on the long term.

Forced and internal variability

The magnitude of internal variability is a strong function of the spatial and temporal scale investigated.

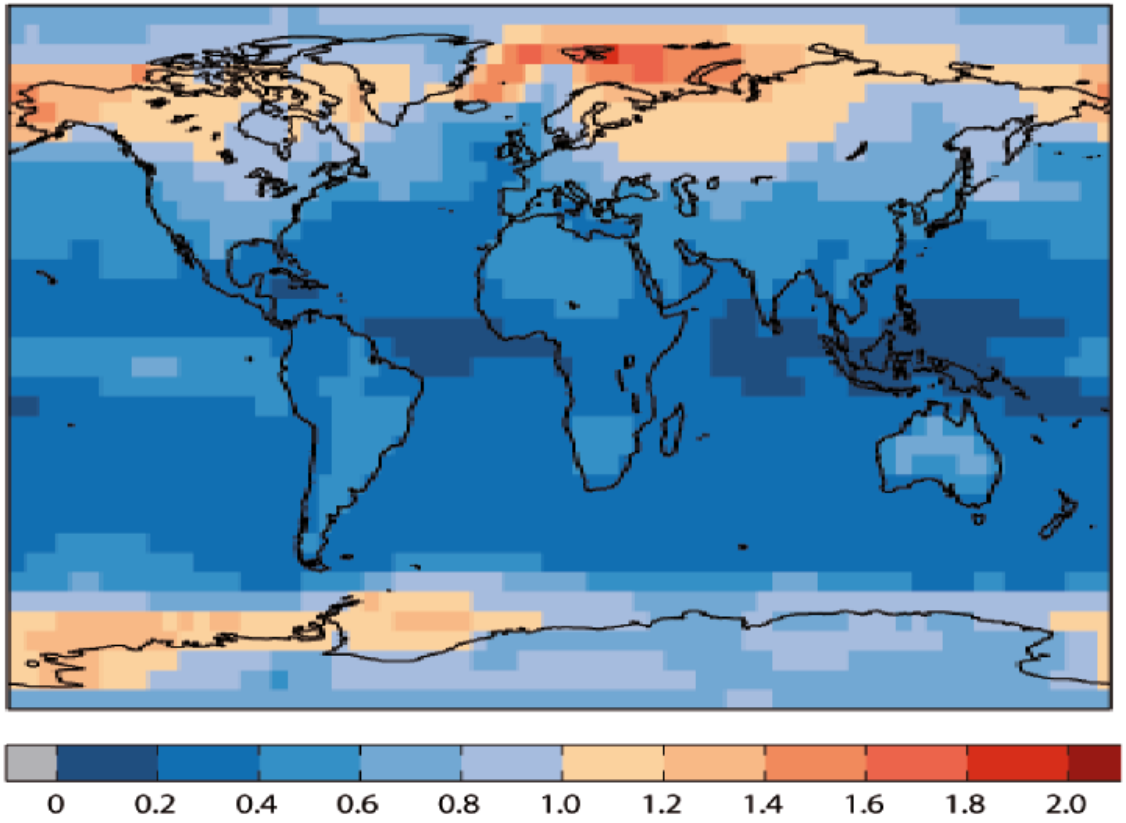

Median of the standard deviation of the annual mean surface air temperature from control simulations performed in the framework of CMIP5. Figure from E. Hawkins updated from Hawkins and Sutton (2012).

Timescales of climate variations

The timescale of climate variations is set up by both the forcing and internal dynamics.

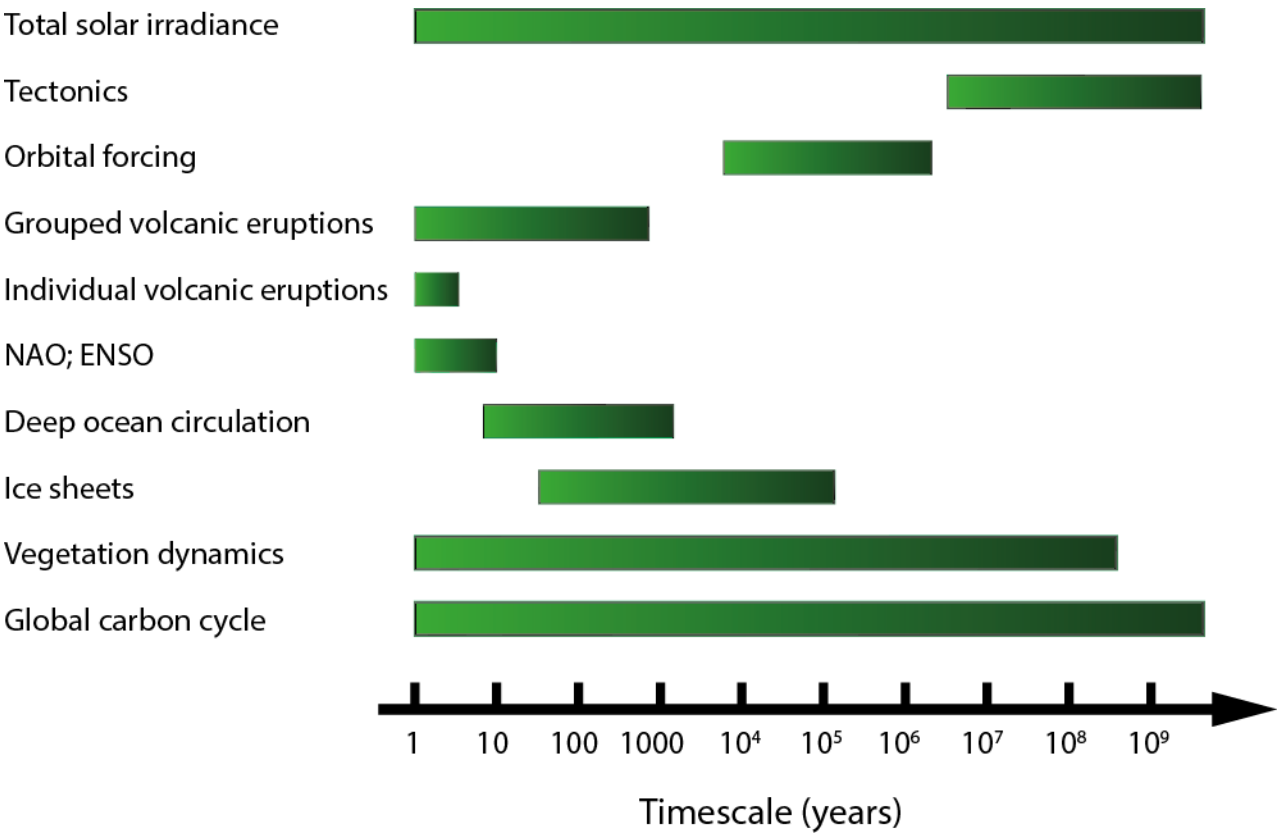

Schematic representation of the dominant timescales of selected external forcing and processes related to internal dynamics which affect climate.

El Niño-Southern Oscillation

In normal conditions, the thermocline is much deeper in the West Pacific than in the East Pacific.

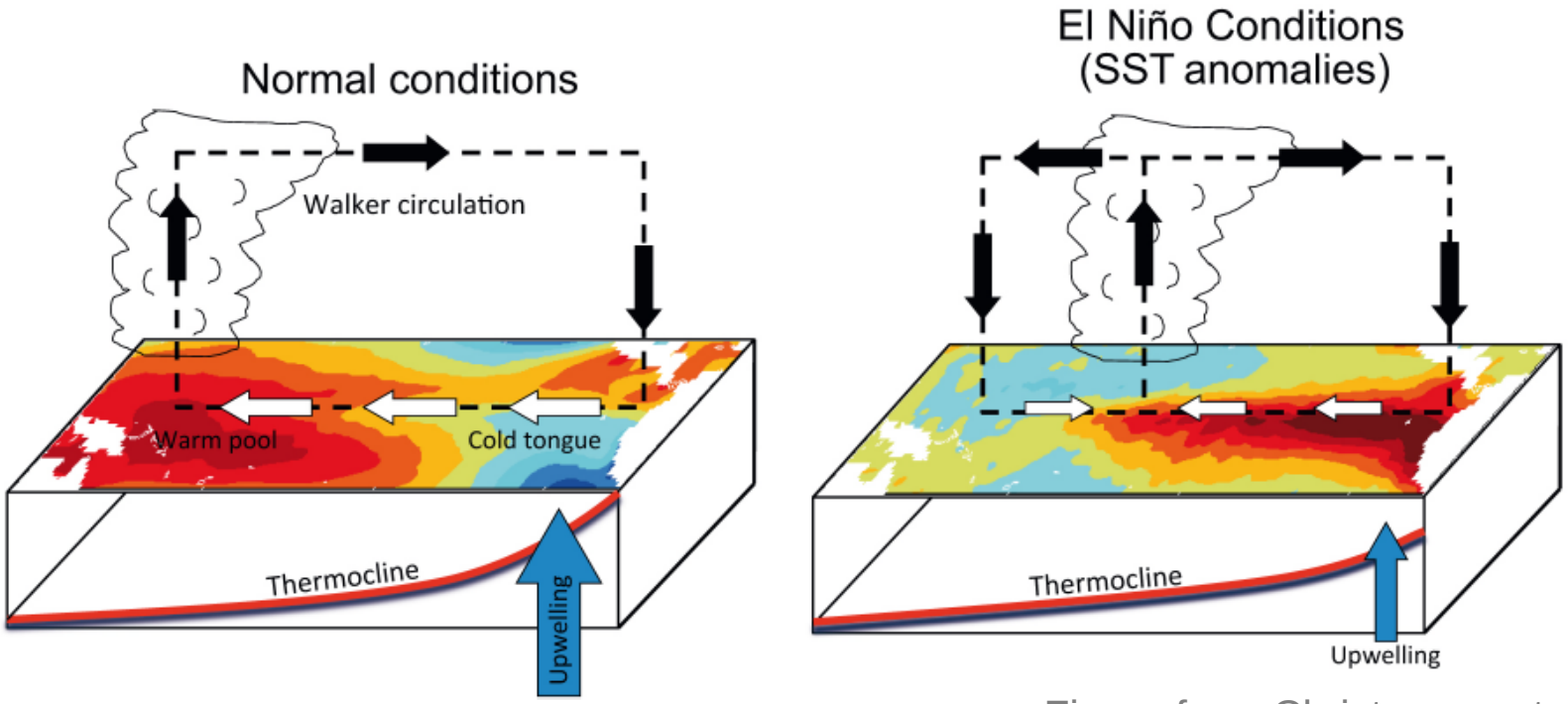

Figure from Christensen et al. (2013)

In El Niño conditions, the intensity of the upwelling is reduced in the East Pacific and the SST warms in the East Pacific.

El Niño-Southern Oscillation

The Walker circulation is associated with a positive feedback, called the Bjerknes feedback.

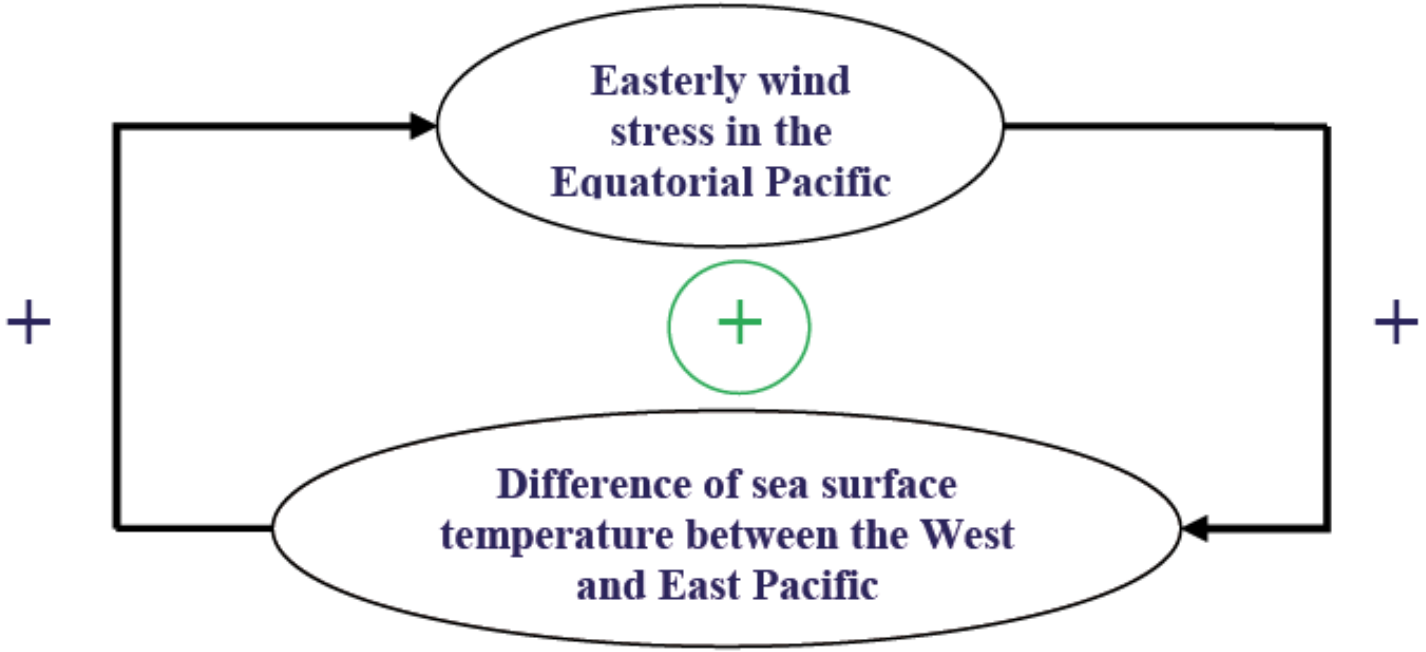

El Niño-Southern Oscillation

The atmospheric circulation and sea surface temperature exhibit irregular oscillations: El Niño Southern Oscillation (ENSO).

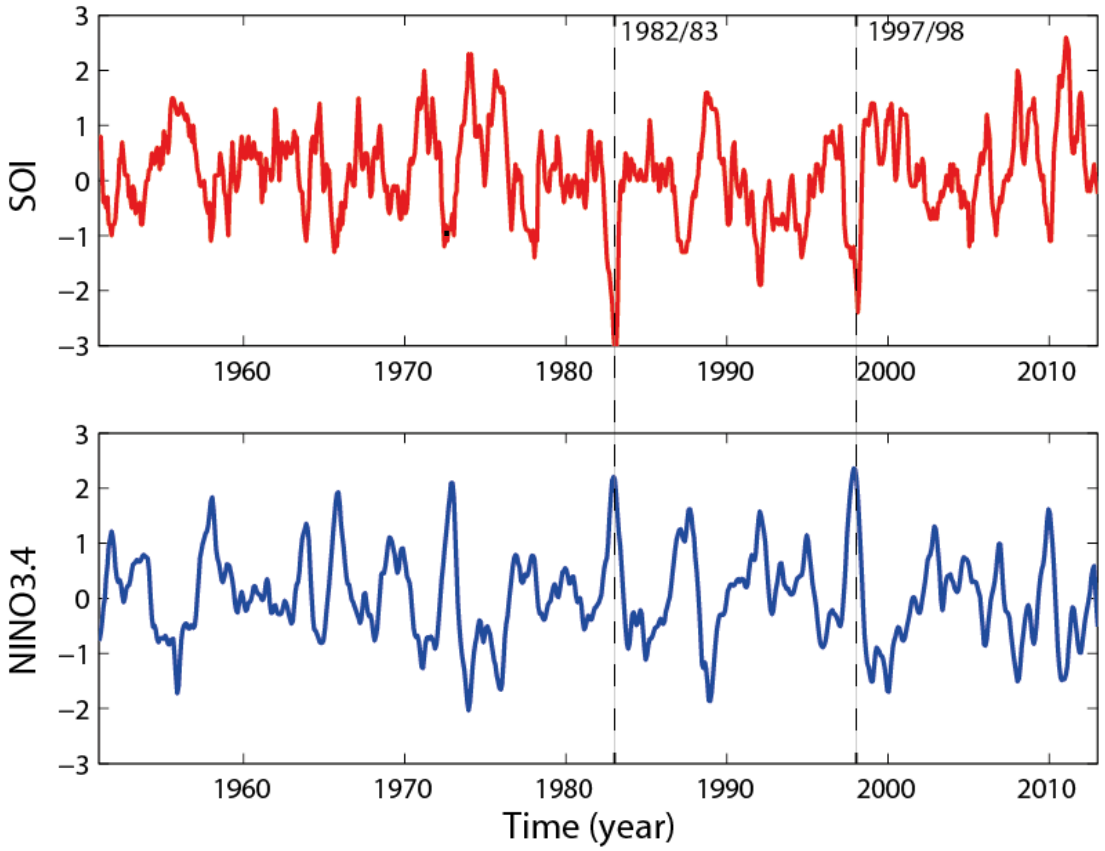

Time series of the temperature in the eastern equatorial Pacific (averaged over the area 5°N-5°S-170°W-120°W, the so-called Niño3.4 index) and the SOI index (normalized difference between SLP in Tahiti and Darwin). Source: http://www.cpc.ncep.noaa.gov/data/indices/

El Niño-Southern Oscillation

ENSO is also associated with nearly global scale perturbations .

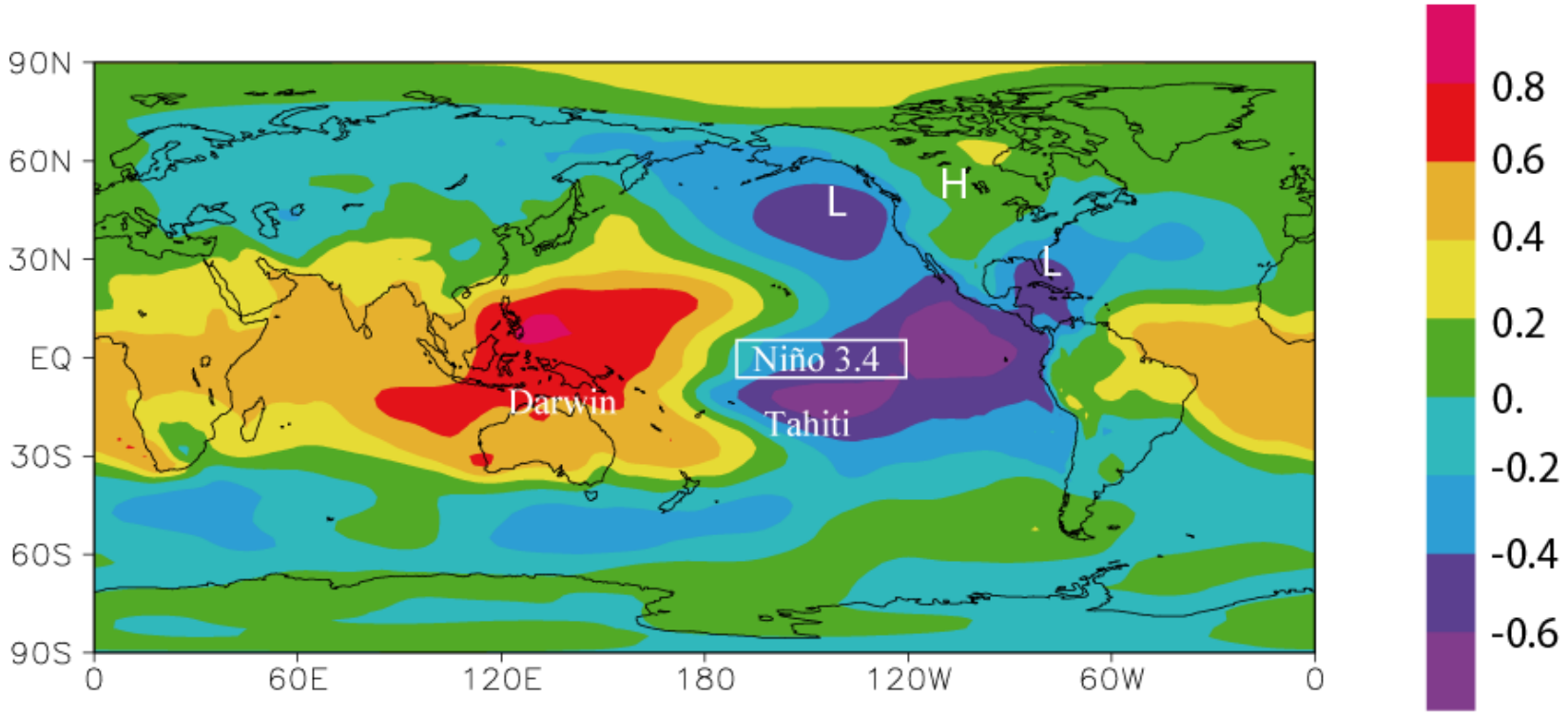

Correlation between the sea surface temperature in the eastern tropical Pacific (Niño3.4 index) and sea-level pressure in January.

The North Atlantic Oscillation

The mid-latitude westerlies in the North Atlantic present irregular changes in their intensity and in the location of their maximum.

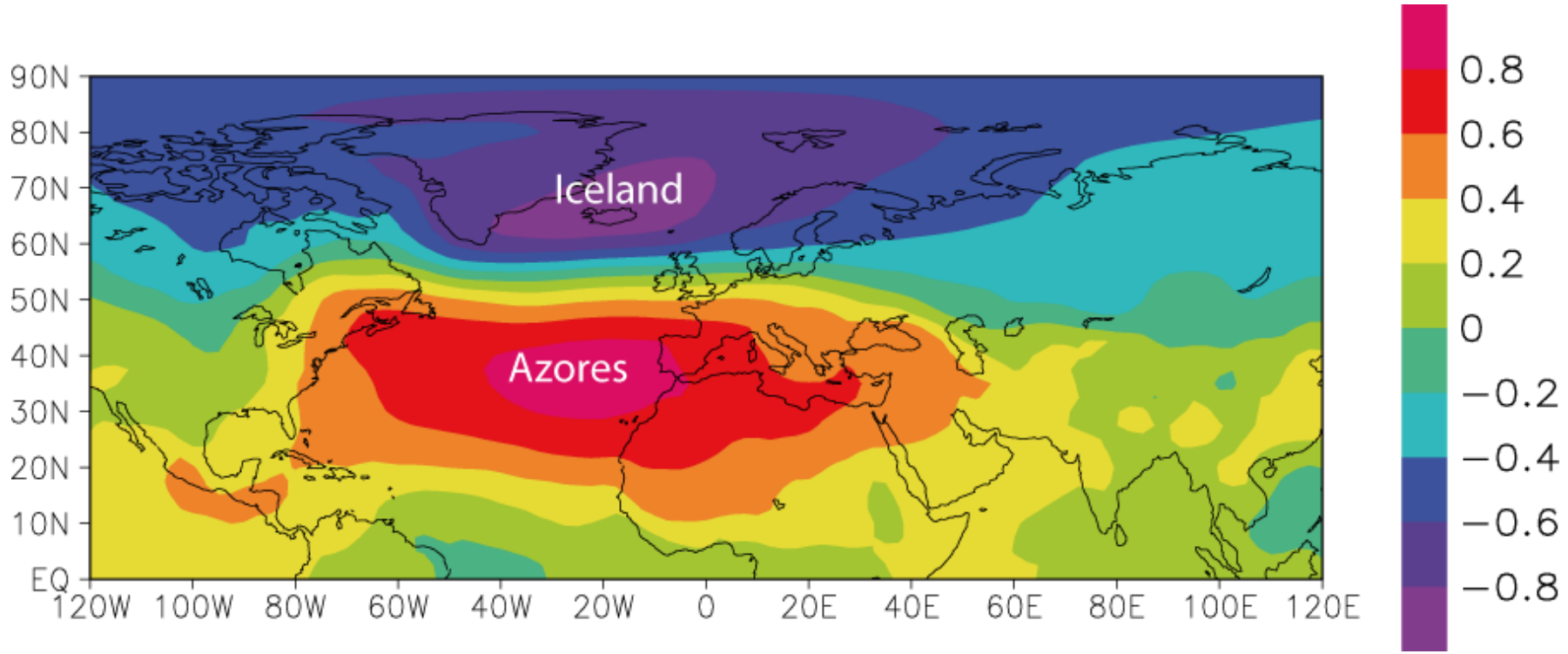

Correlation between the winter NAO index and the winter SLP (average over December, January, February).

The North Atlantic Oscillation

The NAO is associated with changes in many atmospheric and oceanic variables.

Correlation NAO index-winter temperatures

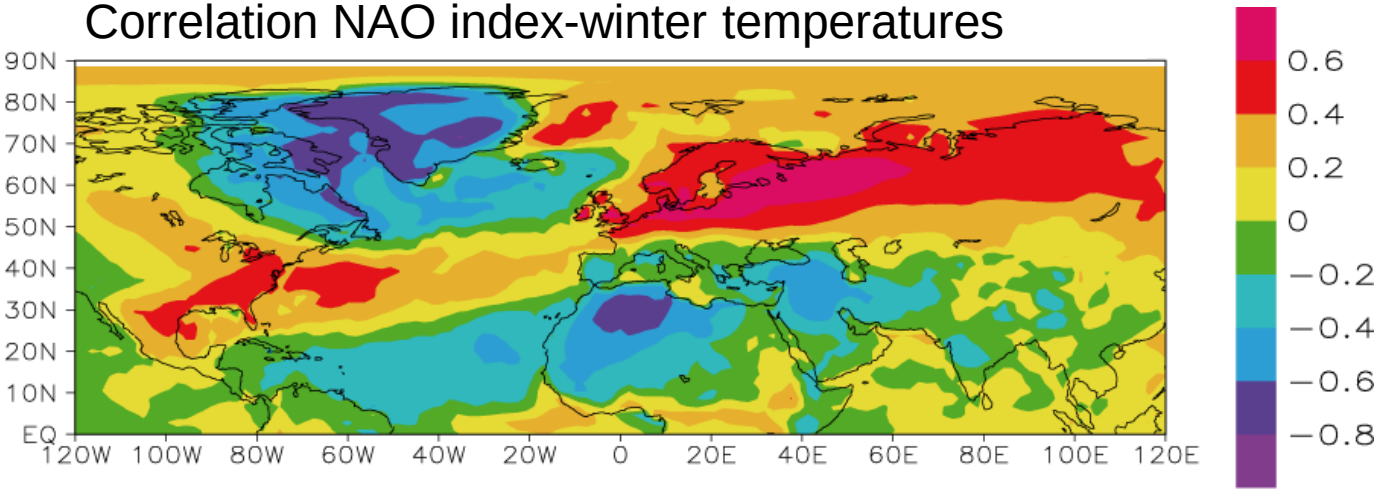

Regression NAO index-winter temperatures

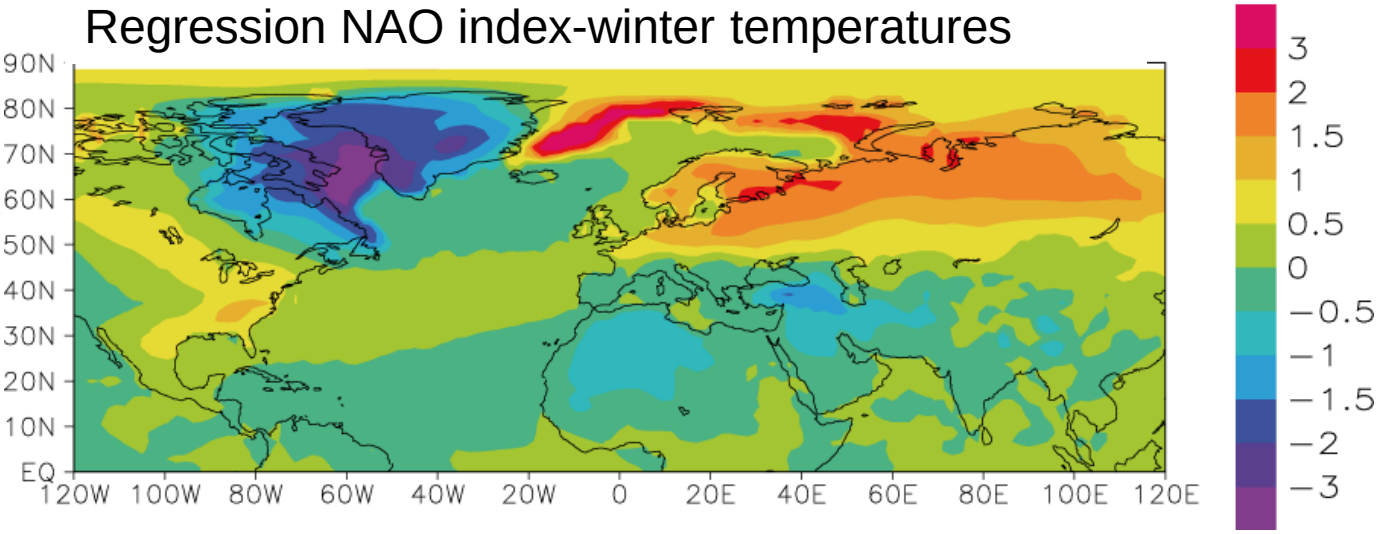

Correlation (top) and regression in °C (bottom) between the winter NAO index and the winter surface air temperature (average over December, January, February).

The Atlantic multidecadal oscillation and the Pacific decadal oscillation

The sea surface temperature is characterized by pronounced decadal and multidecadal variations.

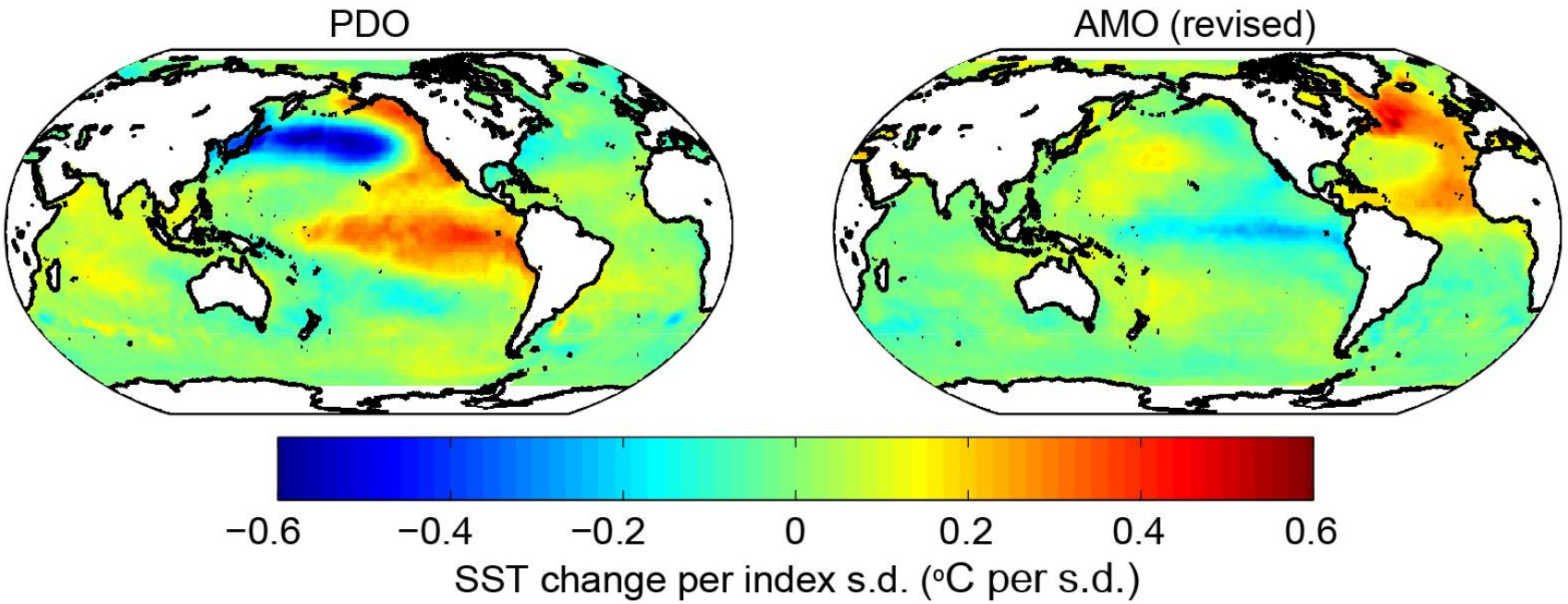

Regression between PDO and AMO indices with annual sea surface temperature. Figure from Hartmann et al. (2014).

Reconstructing past climates

Past climate variations can be reconstructed using the signal recorded in natural archives by various sensors.

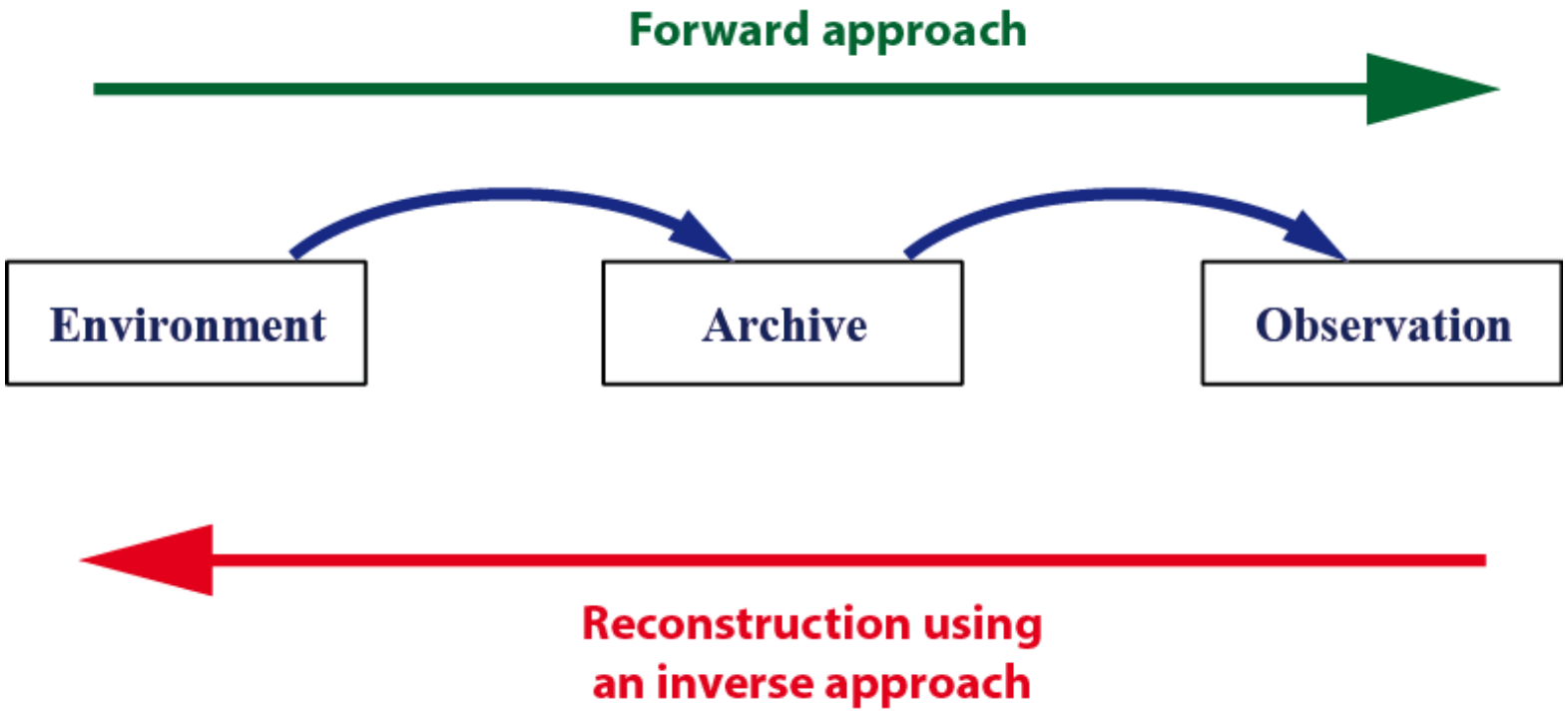

Schematic illustration of the forward and inverse approaches.

Reconstructing past climates

Dating methods

Annual layer counting.

5 cm-long section from the lake sediment of Cape Bounty, East Lake, Nunavut, Canada. Picture from François Lapointe.

Reconstructing past climates

Dating methods

Radiometric dating: based on the decay of radioactive isotopes.

The decay follows a standard law:

$$N = N_0 e^{-\lambda_R t}$$

decay constant of the radioactive isotope

concentration of radioisotopes at time *t*

initial concentration at time *t*=0

Reconstructions based on isotopes

Oxygen isotopes

The abundance of isotopes is measured using the delta value.

$$\delta^{18}O = \left[\frac{\left({}^{18}O / {}^{16}O \right)_{sample}}{\left({}^{18}O / {}^{16}O \right)_{standard}} - 1 \right].1000$$

$\delta^{18}O$ is the ratio of ^{18}O and ^{16}O isotopes in the sample, compared to a standard.

Reconstructions based on isotopes

Oxygen isotopes

Isotopic fractionation takes place during evaporation and condensation

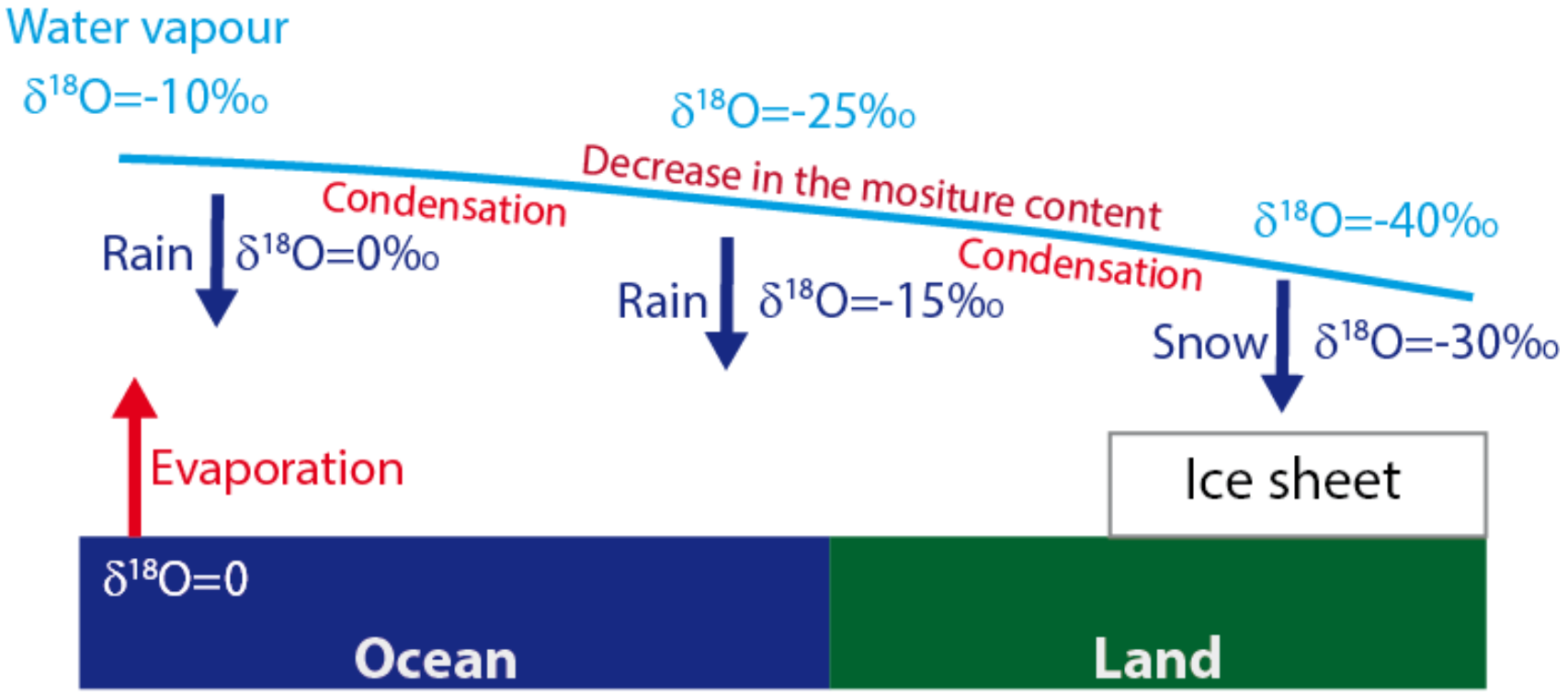

Reconstructions based on isotopes

Carbon isotopes

During photosynthesis, ^{12}C is taken preferentially to ^{13}C because it is lighter.

$$\delta^{13}C = \left[\frac{\left({}^{13}C / {}^{12}C \right)_{sample}}{\left({}^{13}C / {}^{12}C \right)_{standard}} - 1 \right].1000$$

Organic matter has a low (negative) $\delta^{13}C$.

The Climate since the Earth's formation

The uncertainties on Earth' climate are larger as we go back in time.

Eon	Era	Period	Epoch	Date (million years BP)
Phanerozoic	Cenozoic	Quaternary	Holocene	0.012-0
			Pleistocene	2.6-0.012
		Neogene	Pliocene	5.3-2.6
			Miocene	23-5.3
		Paleogene	Oligocene	34-23
			Eocene	56-34
			Paleocene	66-56
	Mesozoic	Cretacious		145-66
		Jurassic		201-145
		Triassic		252-201
	Paleozoic	Permian		299-252
		Carboniferous		359-299
		Devonian		419-359
		Silurian		443-419
		Ordovician		485-443
		Cambrian		541-485
Precambrian	Proterozoic			2500-541
	Archean			4000-2500
	Hadean			4600-4000

A simplified geological time scale.

Precambrian climate

4 billion years ago, the solar irradiance was about 25-30% lower than at present but the Earth was not totally ice covered : the "faint young Sun paradox".

Main hypothesis: a much stronger greenhouse effect caused by a much higher CO_2 (250 times the present-day value?) and CH_4 concentration.

Precambrian climate

Atmospheric composition has been modified with time.

The photosynthesis induced a large increase in the atmospheric oxygen concentration 2.2. to 2.4 billion years ago.

This caused a glaciation ?

Precambrian climate

Large glaciations took place around 550 to 750 million years ago.

Formation of a Snowball Earth around 635 million years ago?

If this is really occurred, why does not Earth not stay permanently in this state ?

Phanerozoic climate

The carbon cycle and climate appear strongly linked on timescales of millions of years.

Changes in atmospheric CO_2 concentration can be represented by:

$$\frac{\partial [CO_2]}{\partial t} = Volc(t) - \left(Weath(t) + Org(t)\right)$$

Outgassing of CO_2 due to metamorphism and volcanic eruptions

Silicate weathering and calcium carbonate sedimentation in the ocean

Long-term burial of organic matter

Phanerozoic climate

The models based on this balance are able to reproduce the long term changes in the carbon cycle.

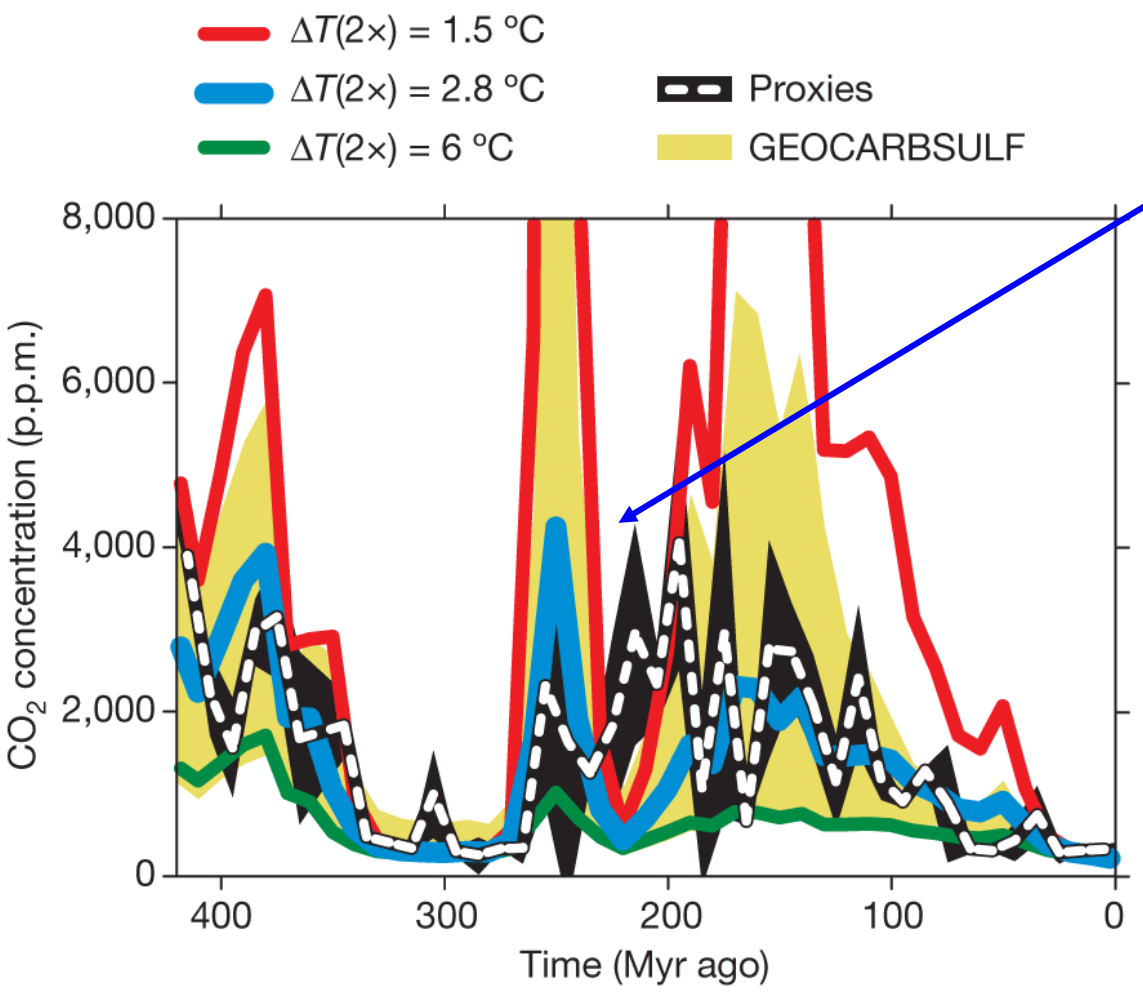

Large influence of climate sensitivity

Comparison of the CO_2 concentration calculated by GEOCARBSULF model for varying climate sensitivities (noted $\Delta T(2x)$ on the figure) to an independent CO_2 record based on different proxies. Figure from Royer et al. (2007).

Cenozoic climate

The temperature over the last 65 million years has gradually decreased . This is associated with a cooling that is often referred to as a transition from a greenhouse climate to an icehouse.

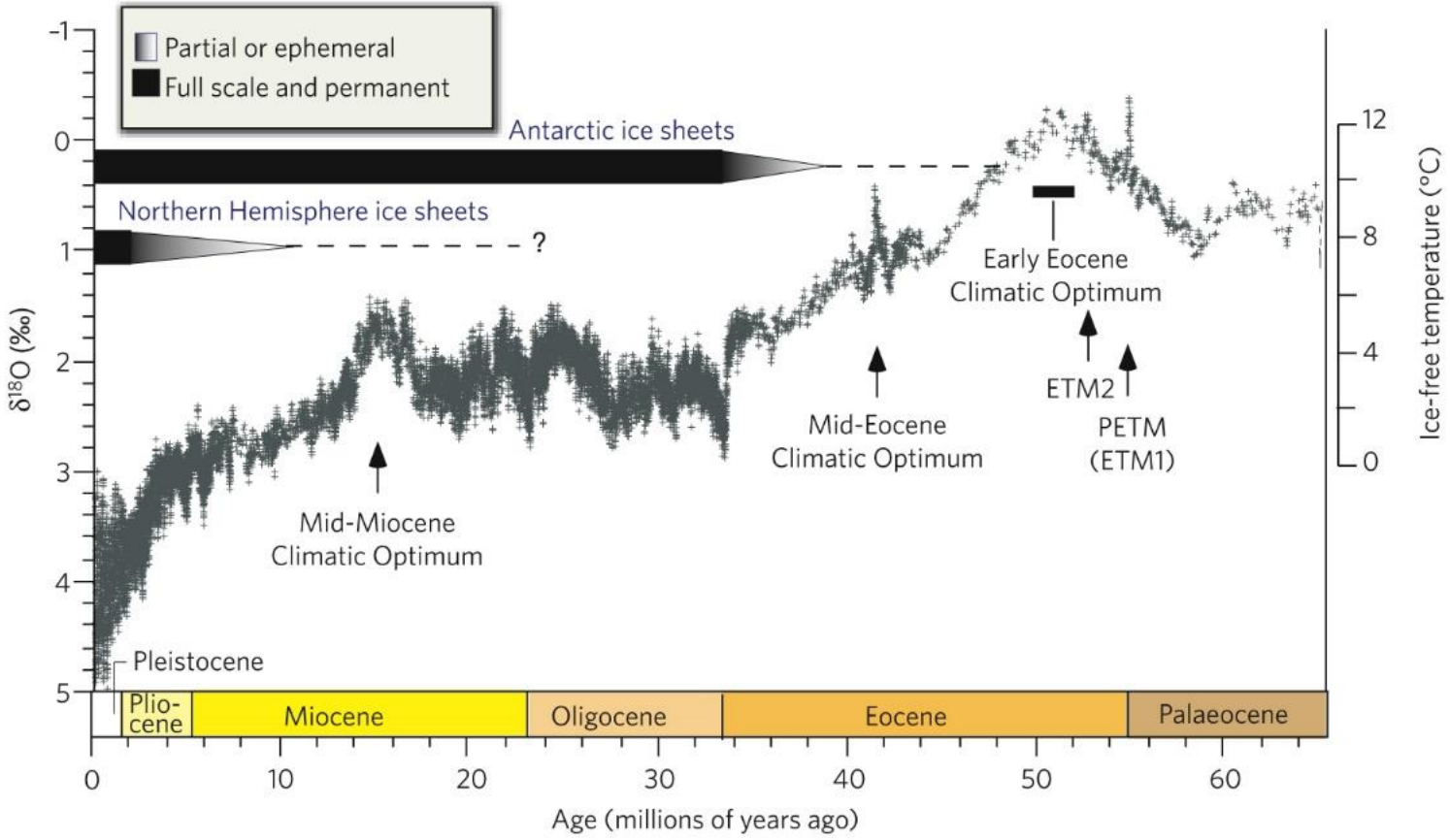

The global climate over the past 65 million years based on deep-sea oxygen-isotope measurements. Figure from Zachos et al. (2008).

Cenozoic climate

During the Paleocene Eocene Thermal Maximum (PETM, 55 million years ago) global temperature increased by more than 5°C in about 10 000 years.

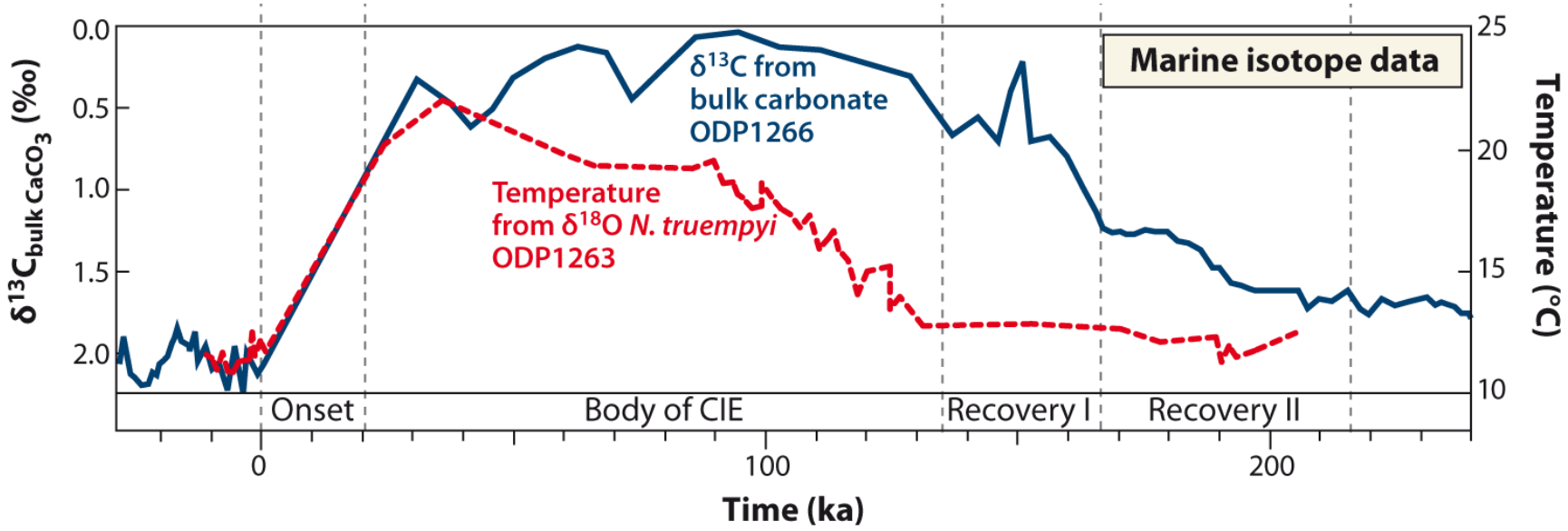

Carbonate carbon isotope and oxygen isotope ratio in two cores in the South Atlantic. The time on the x axis starts at the onset of the PETM about 55 million years ago. Figure from McInerney and Wing (2011).

Cenozoic climate

50 million years ago, the location of the continents was quite close to that of the present-day one but changes in boundary conditions still had an influence on climate.

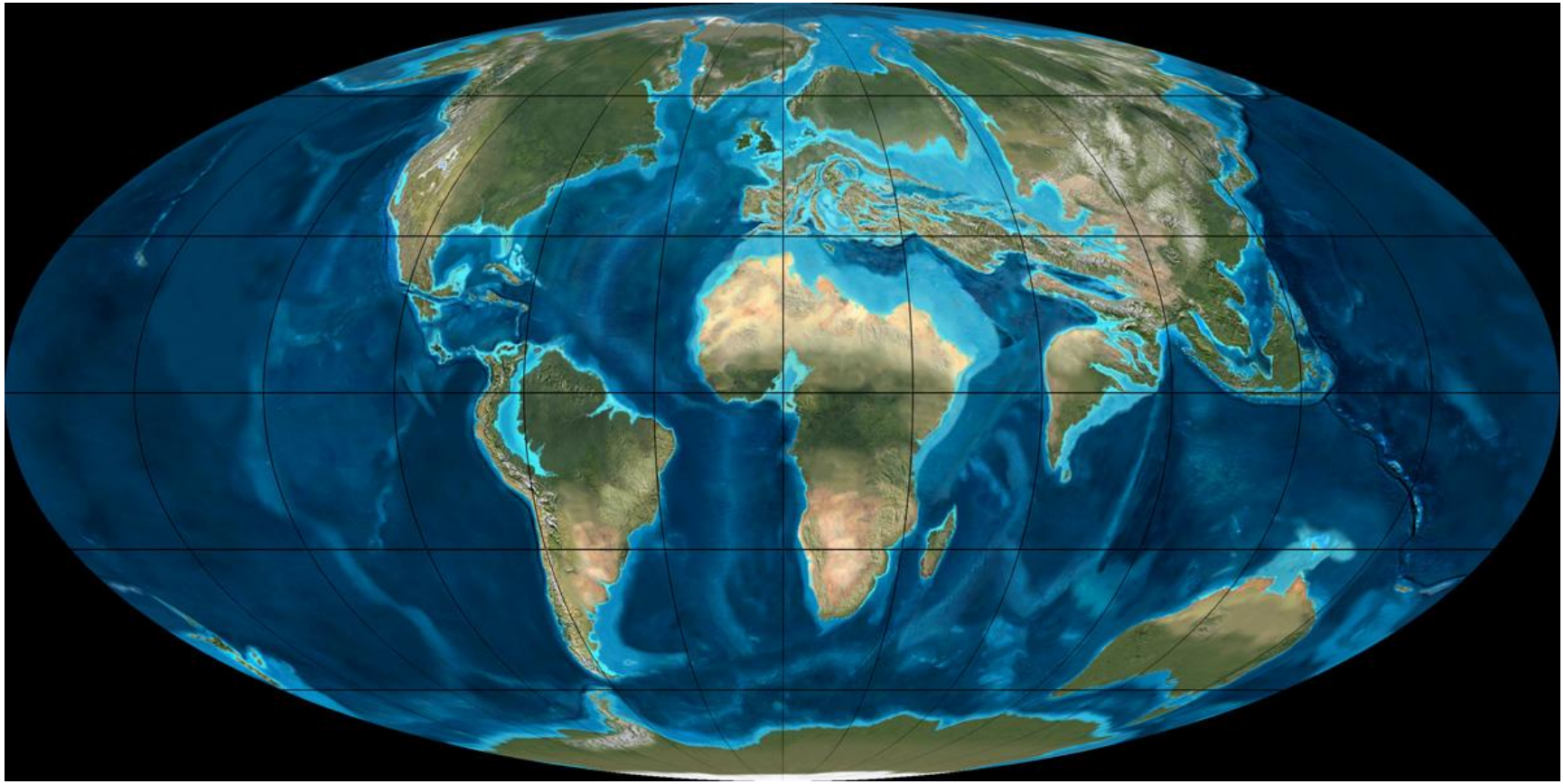

Land configuration about 60 million years ago. Map from Ron Blakey

Cenozoic climate

Large climate fluctuations have occurred over the last 5 million years.

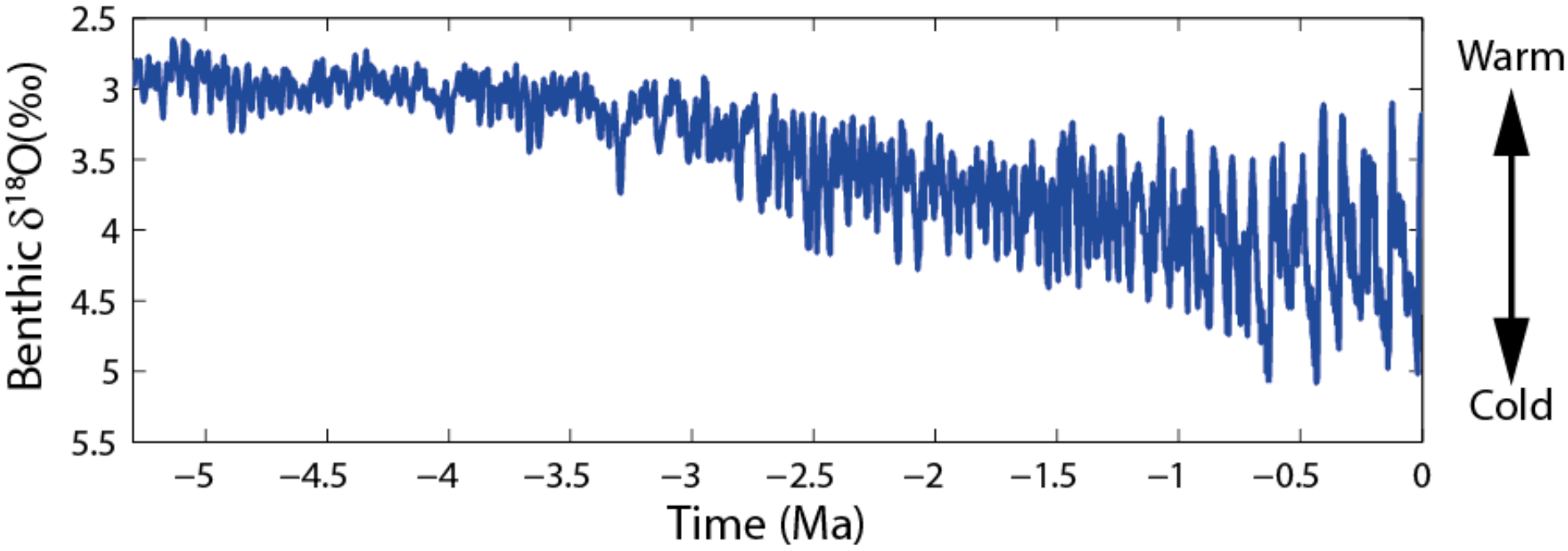

Benthic δ18O, which measures global ice volume and deep ocean temperature. Data from Lisiecki and Raymo (2005).

The last million years: glacial interglacial cycles

The characteristics of the Earth's orbit are determined by three astronomical parameters.

eccentricity (*ecc*)

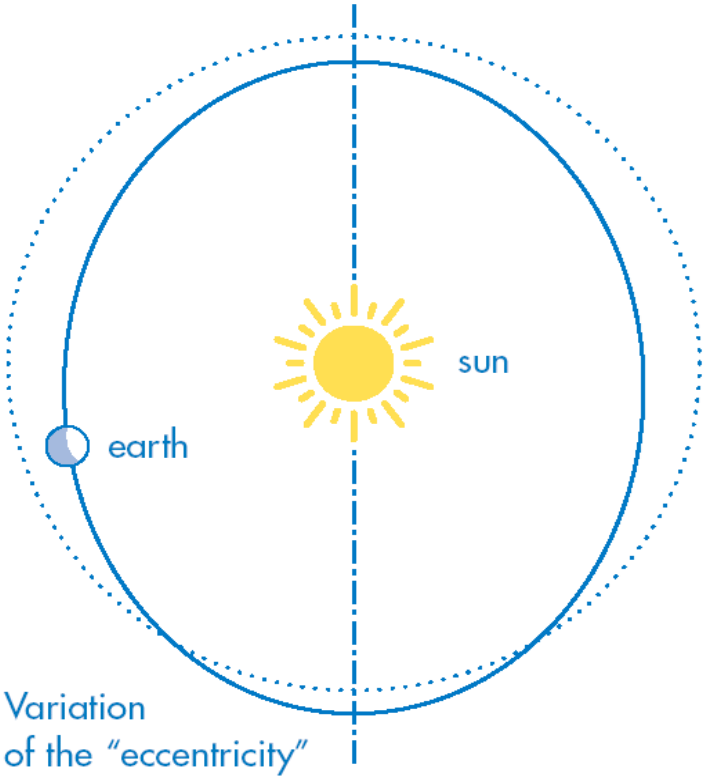

obliquity (ε_{obl}),

The last million years: glacial interglacial cycles

The climatic precession is *ecc sin (PERH) = ecc sin (ω)*

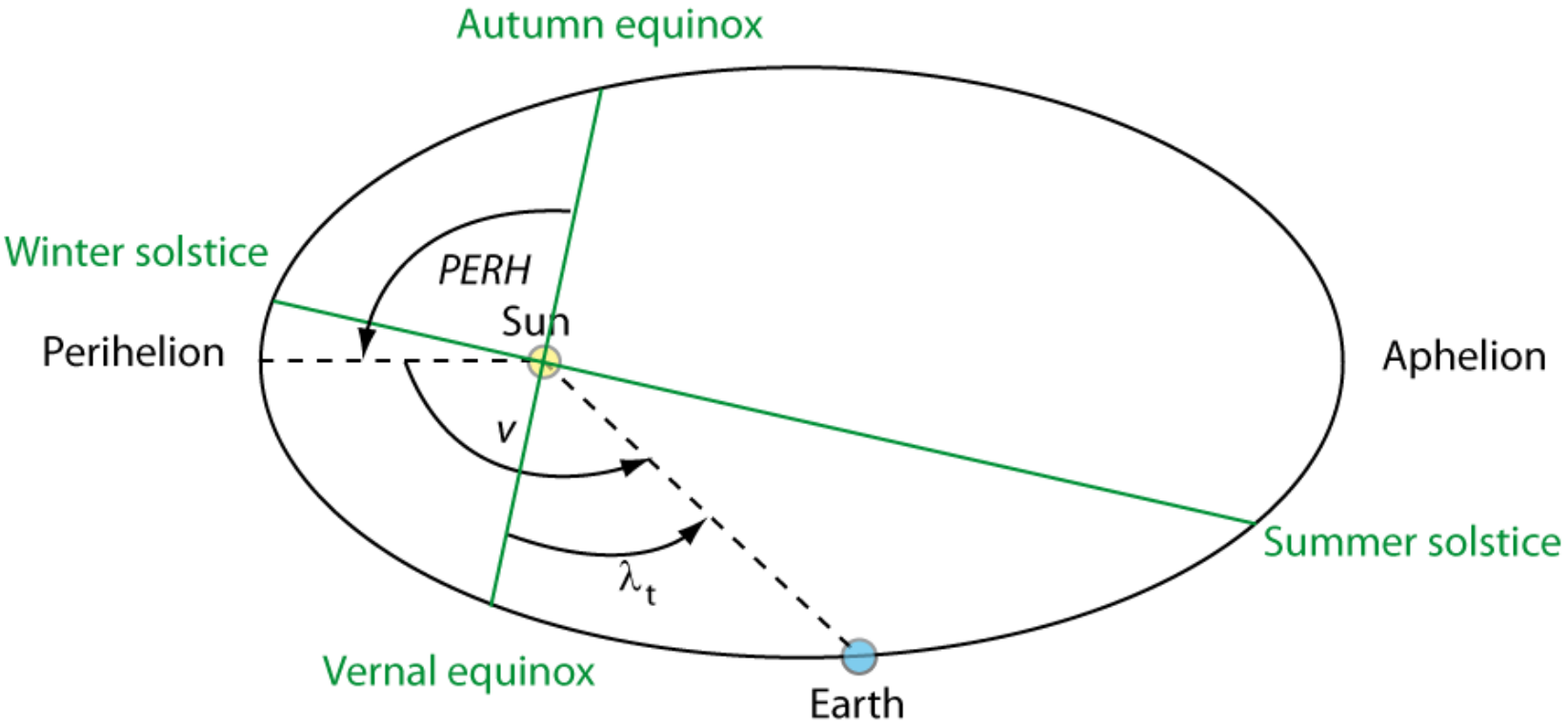

The last million years: glacial interglacial cycles

Because of the climatic precession, the Earth was closest to the sun during the boreal summer 11 ka ago and the closest to the sun during boreal winter now.

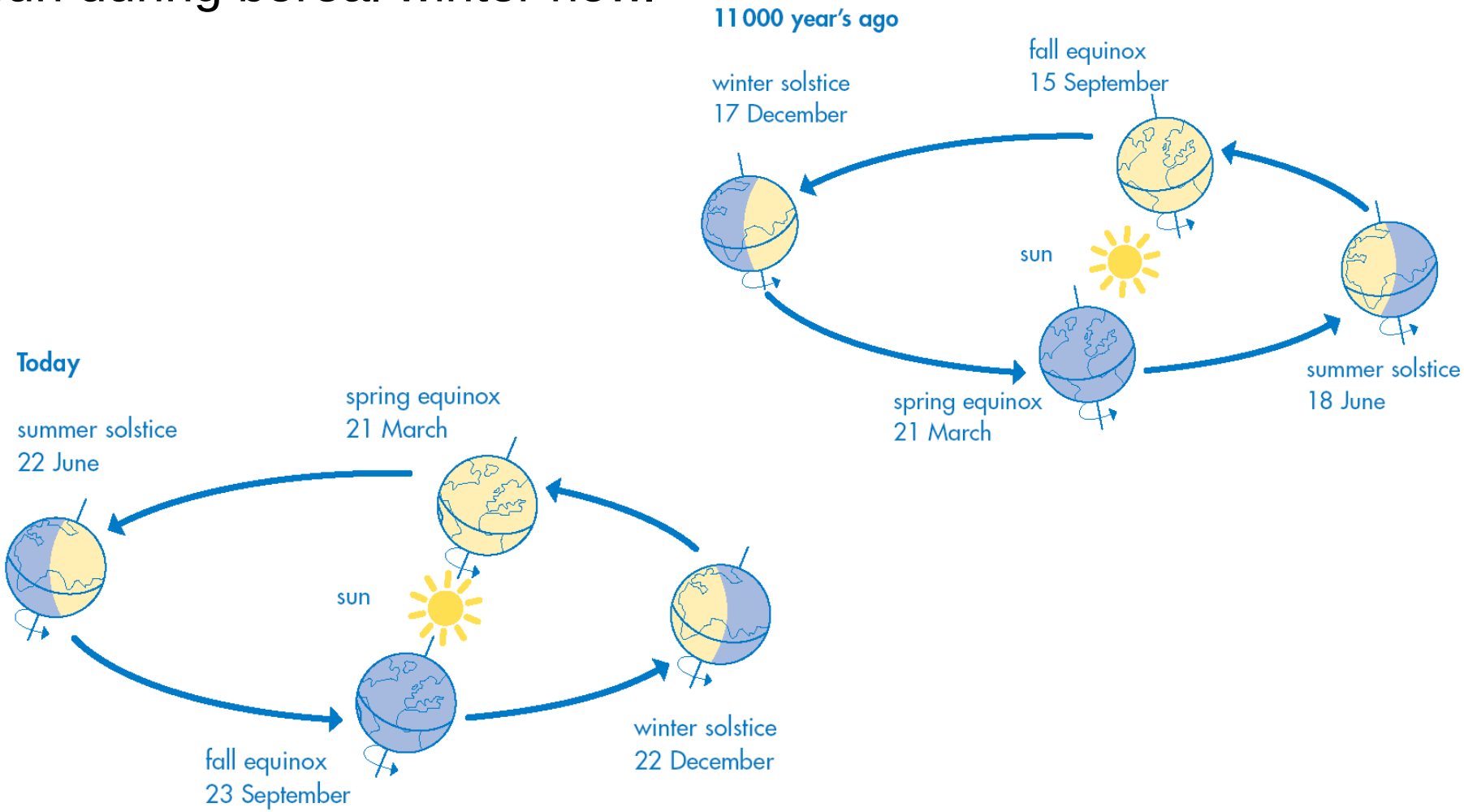

The last million years: glacial interglacial cycles

The astronomical parameters are varying through time.

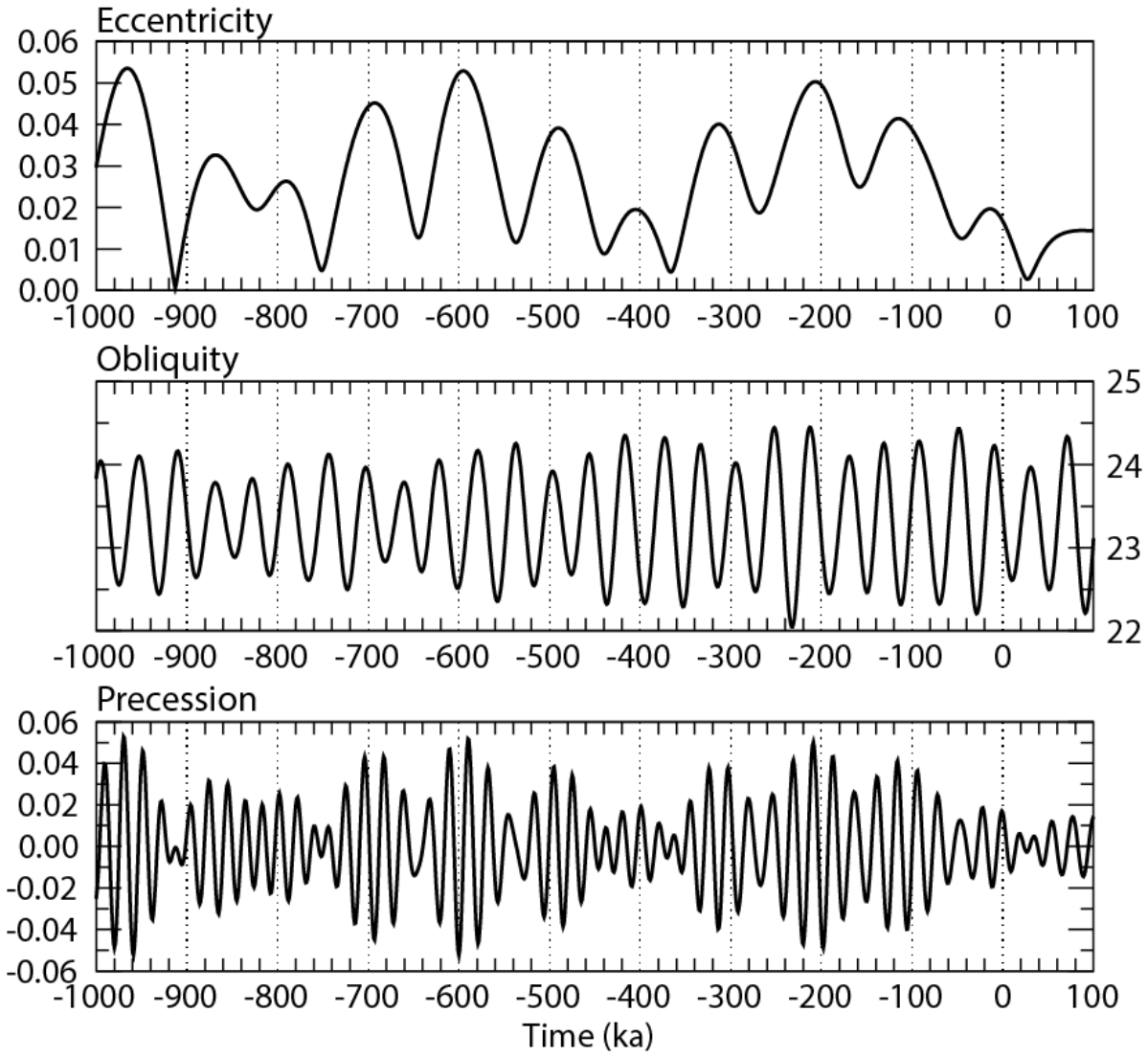

Long-term variations in eccentricity, climatic precession and obliquity (in degrees). zero corresponds to 1950 AD. Computed from Berger (1978). Figure from Marie-France Loutre.

The last million years: glacial interglacial cycles

Eccentricity. The annual mean energy received by the Earth is inversely proportional to:

$$\sqrt{\left(1-ecc^2\right)}$$

The differences in the annual mean radiations received by the Earth are small: maximum variation of 0.15%, i.e., 0.5 W m^{-2} .

The last million years: glacial interglacial cycles

The **obliquity** has a large impact on the seasonal distribution of insolation in polar regions.

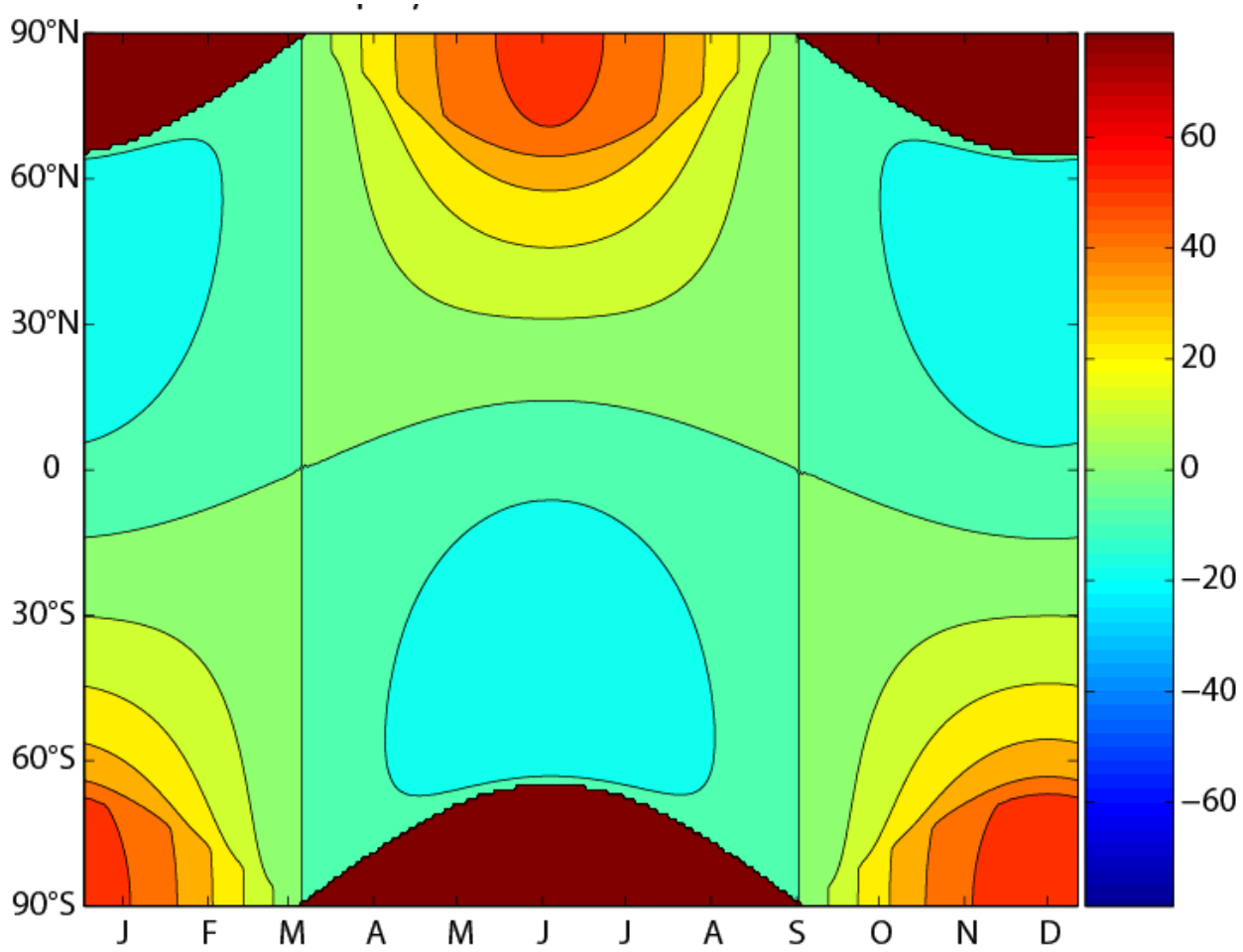

Changes in insolation in W m^{-2} caused by an increase in the obliquity from 22.0° to 24.5° with *ecc*=0.016724, PERH=102.04, i.e. the present-day values. Figure from Marie-France Loutre

The last million years: glacial interglacial cycles

The **climatic precession** has a large impact on the seasonal cycle of insolation.

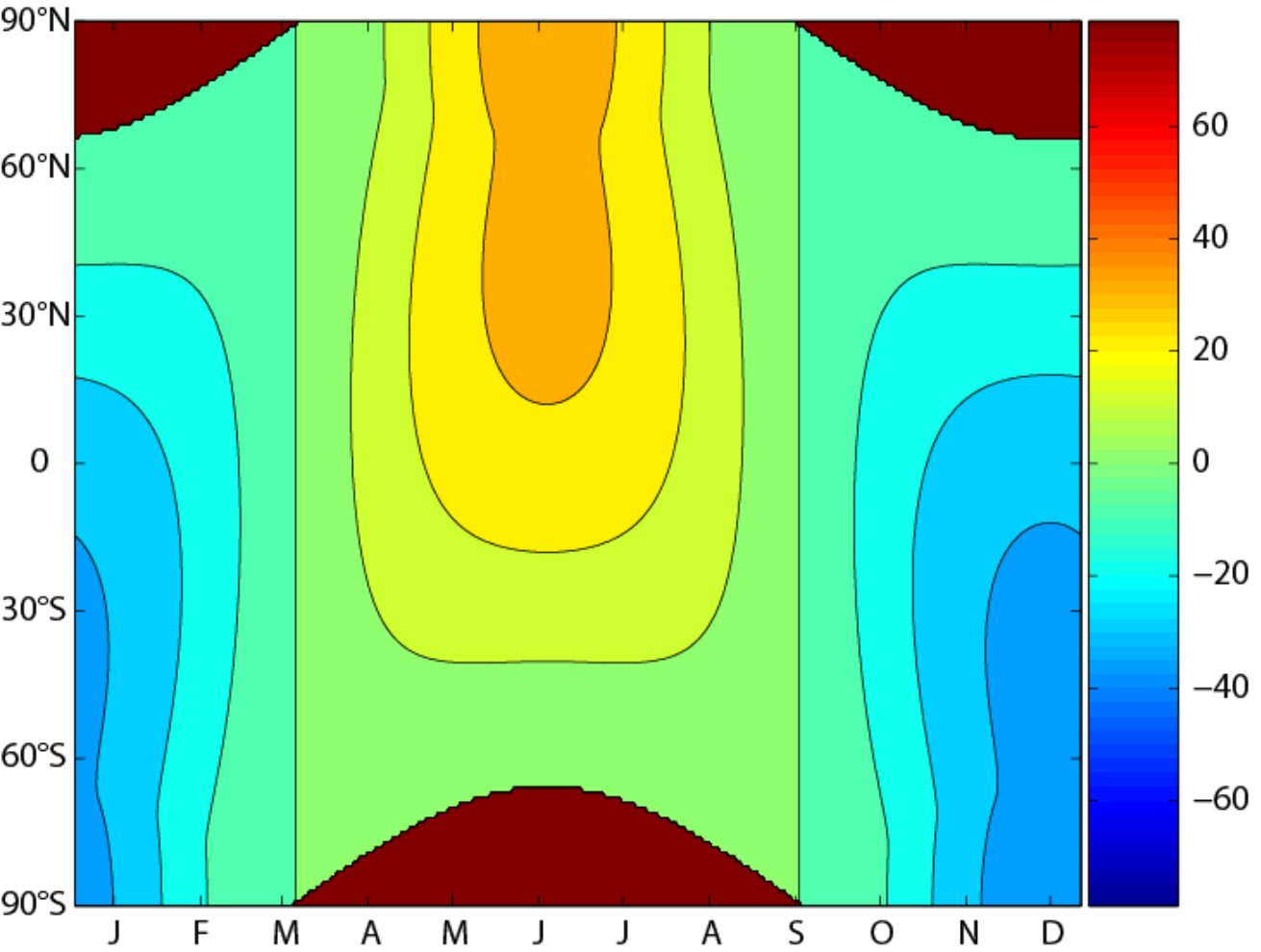

Changes in insolation in W m^{-2} caused by a decrease of the climatic precession from its maximum value (boreal winter at perihelion) to its minimum value (boreal summer at perihelion) with *ecc*=0.016724, ε_{obl}=23.446°, i.e. the present-day values. Figure from Marie-France Loutre

The last million years: glacial interglacial cycles

The last 800 kyr are characterized by the alternation between long glacial periods and relatively brief interglacials.

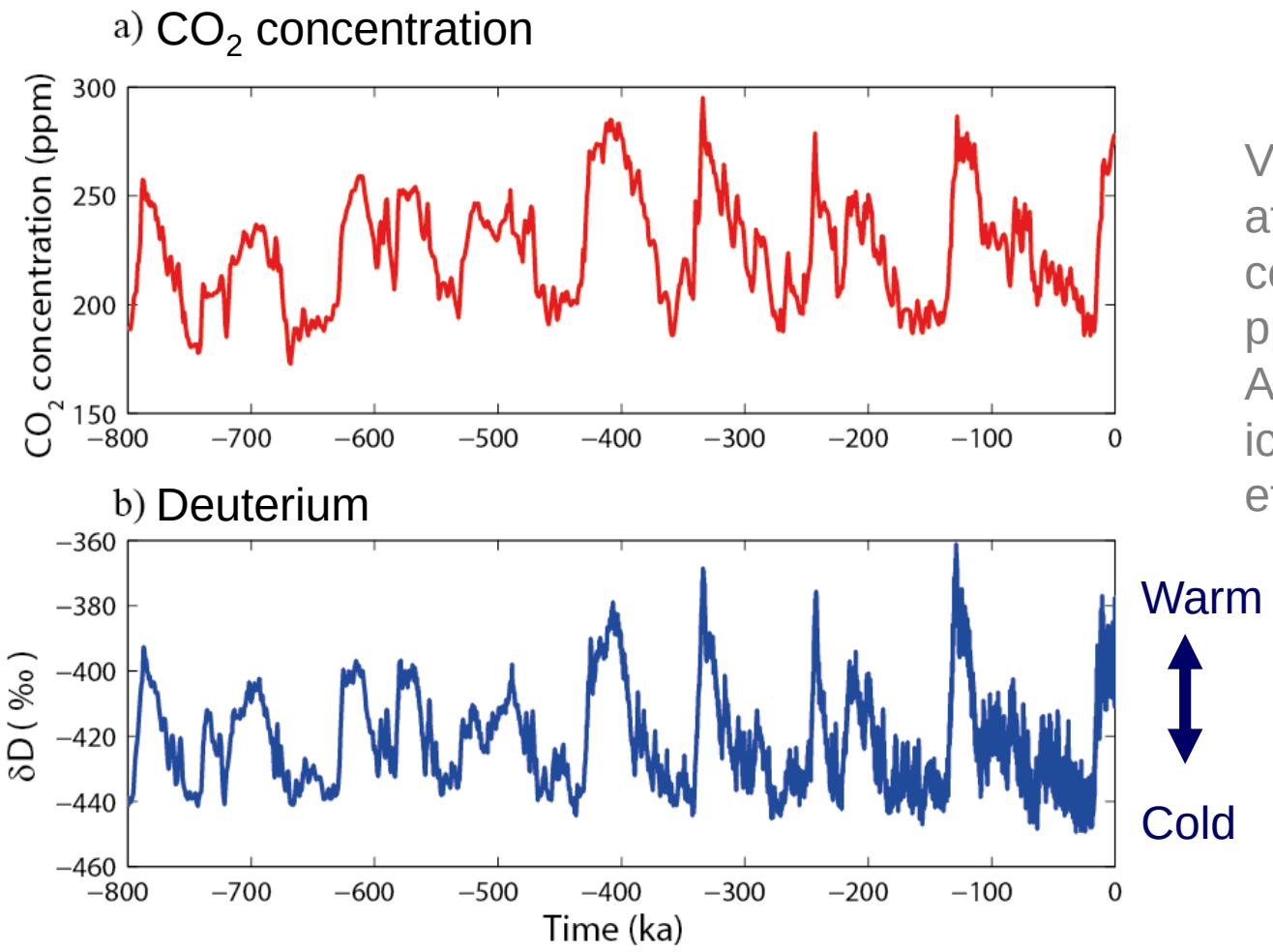

Variations in the atmospheric concentrations of CO_2 (in ppm, and in deuterium in Antarctica Dome C (EDC) ice core (δD in ‰, Jouzel et al., 2007).

The last million years: glacial interglacial cycles

The latest glacial period culminates about 21 ka ago: the Last Glacial Maximum (LGM).

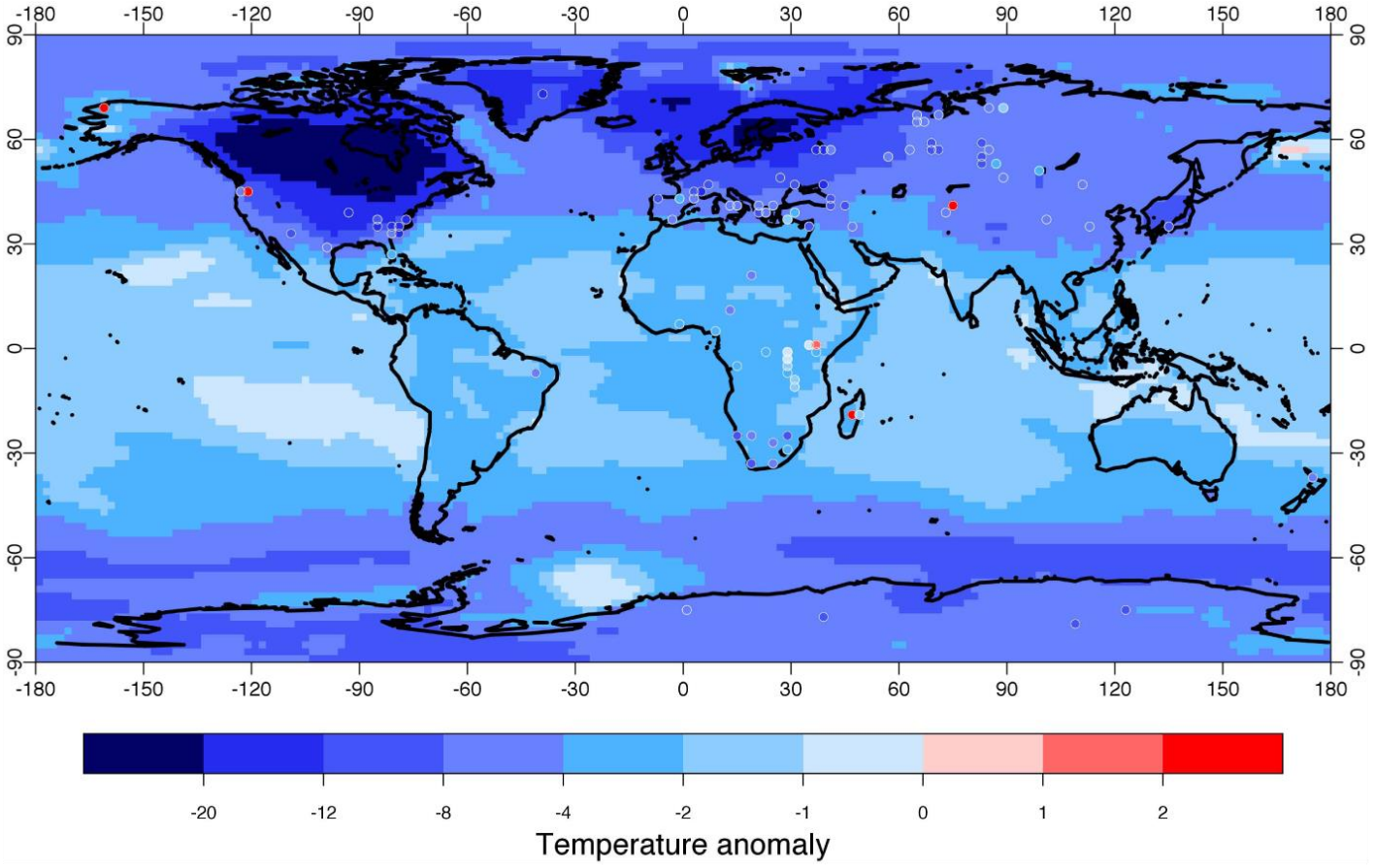

Reconstruction of the difference in surface air temperature between the Last Glacial Maximum and preindustrial conditions. Figure from Annan and Hargreaves (2013).

The last million years: glacial interglacial cycles

The astronomical theory of paleoclimate assumes that glacial interglacial-cycles are driven by the changes in the astronomical parameters.

The summer insolation at high northern latitudes appears to be of critical importance.

The last million years: glacial interglacial cycles

The astronomical theory of paleoclimate.

The dominant frequencies of the astronomical parameters are also found in many proxy records of past climate changes.

Models driven by past changes in orbital parameters and by the observed evolution of greenhouse gases reproduced quite well the estimated past ice volume variations .

However, the link between climate change and insolation is far from being simple and linear.

The last million years: glacial interglacial cycles

The astronomical theory of paleoclimate.

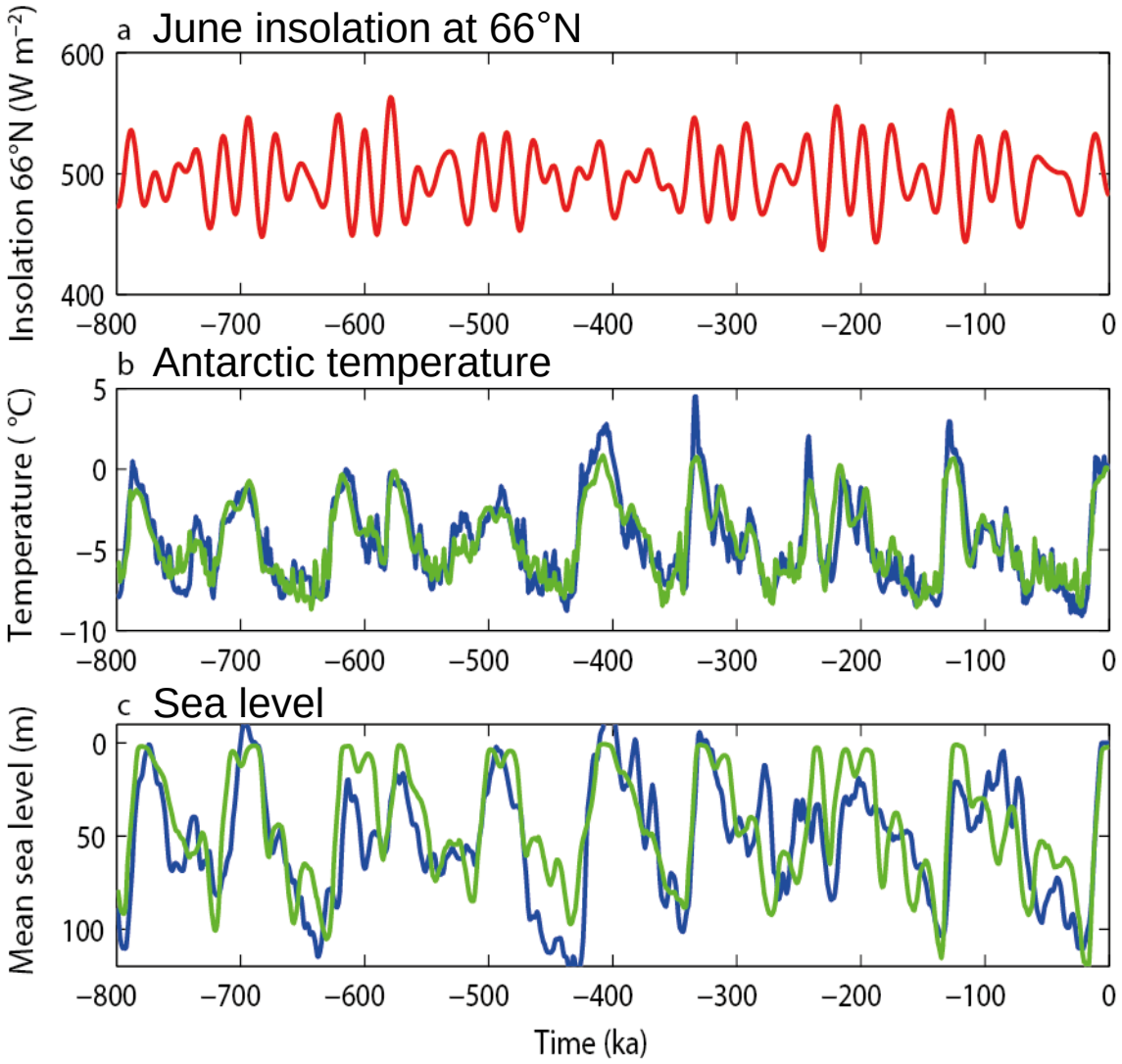

Insolation at 66°N at the June solstice (in W m^{-2}, red) according to Berger (1978), anomaly of Antarctic temperature reconstructed from the deuterium record (blue) and in the simulation of Ganopolski and Calov (2011) (green), Sea level reconstructed by Elderfield et al. (2012) (blue) and deduced from the change in continental ice volume simulated in Ganopolski and Calov (2011) (green).

Observation

Model

The last million years: glacial interglacial cycles

The glacial-interglacial variations in the atmospheric CO_2 concentration reach 90 ppm.

This corresponds to a radiative forcing of 2 W m^{-2}.

Mechanisms contributing to the glacial to interglacial difference in CO_2.

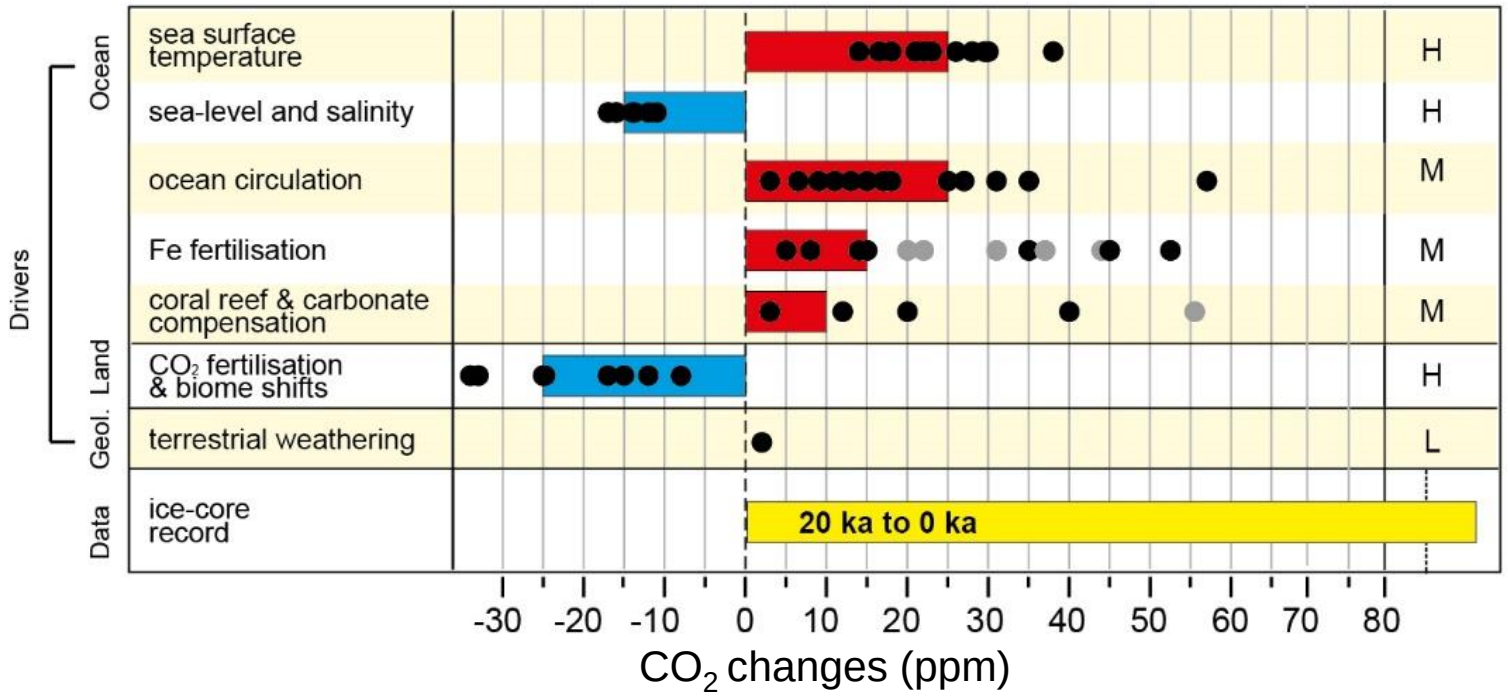

Figure from Ciais et al. (2013).

Millennial-scale variability during glacial periods

Dansgaard-Oeschger events are abrupt events characterized by warming in Greenland of several degrees in a few decades.

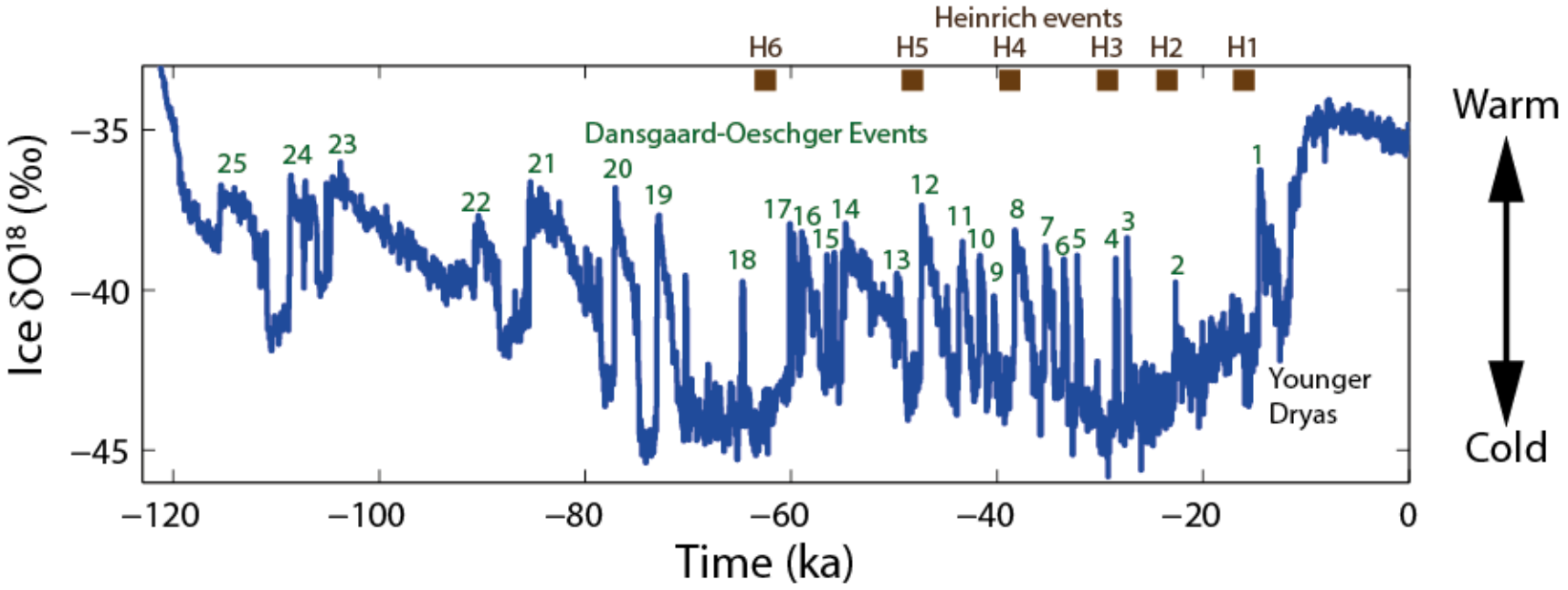

Time series of $\delta^{18}O$ measurements obtained in the framework of the North Greenland Ice Core Project (NGRIP, North Greenland Ice Core Project Members, 2004).

Dansgaard-Oeschger events have a global impact.

Millennial-scale variability during glacial periods

Heinrich events correspond to a massive iceberg discharge that let thick layers of debris in the sediments of the North Atlantic.

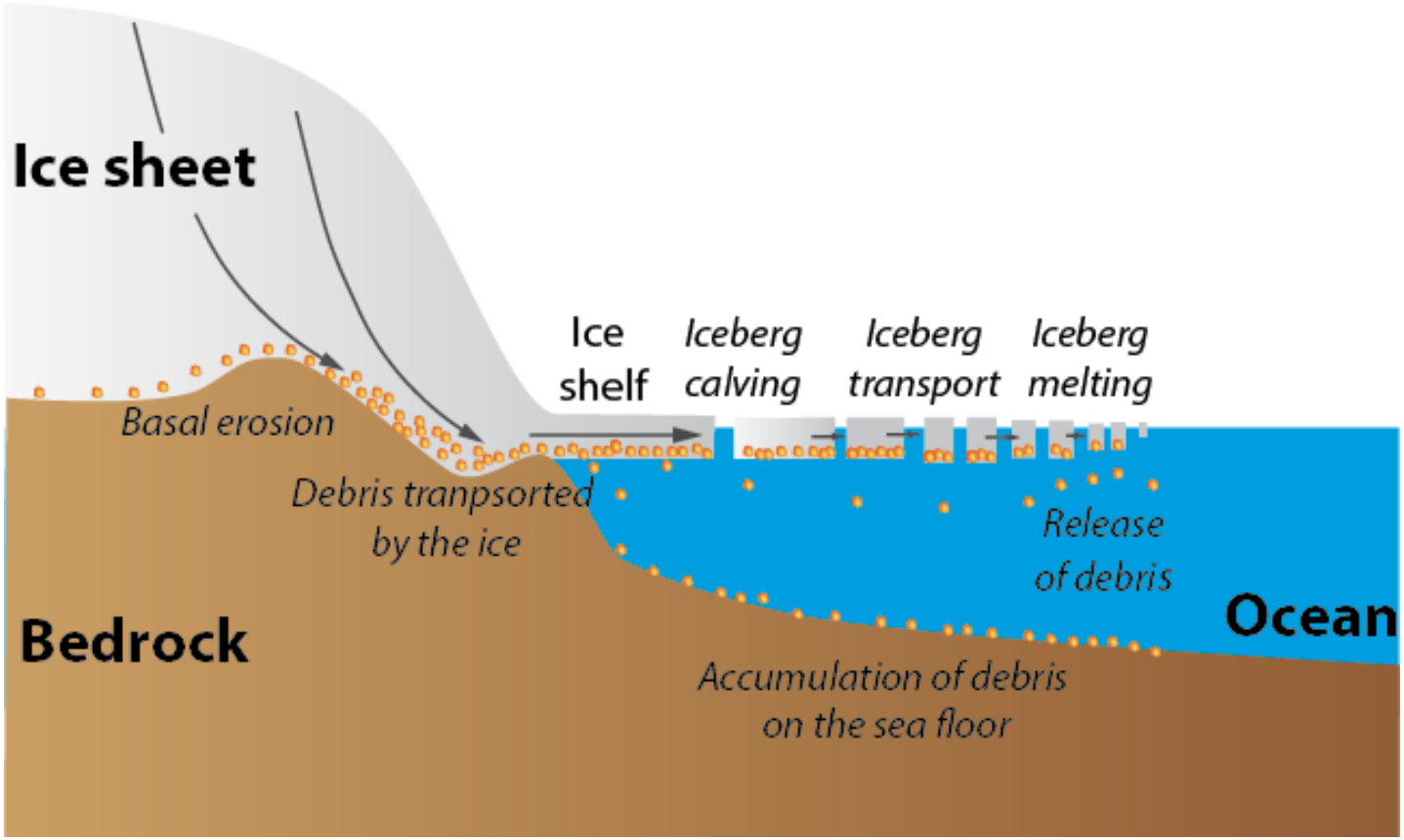

Schematic representation of the massive iceberg release leading to the sediments deposits characteristics of Heinrich events.

Millennial-scale variability during glacial periods

The millennial-scale variability is likely related to the ice sheet dynamics and the oceanic circulation.

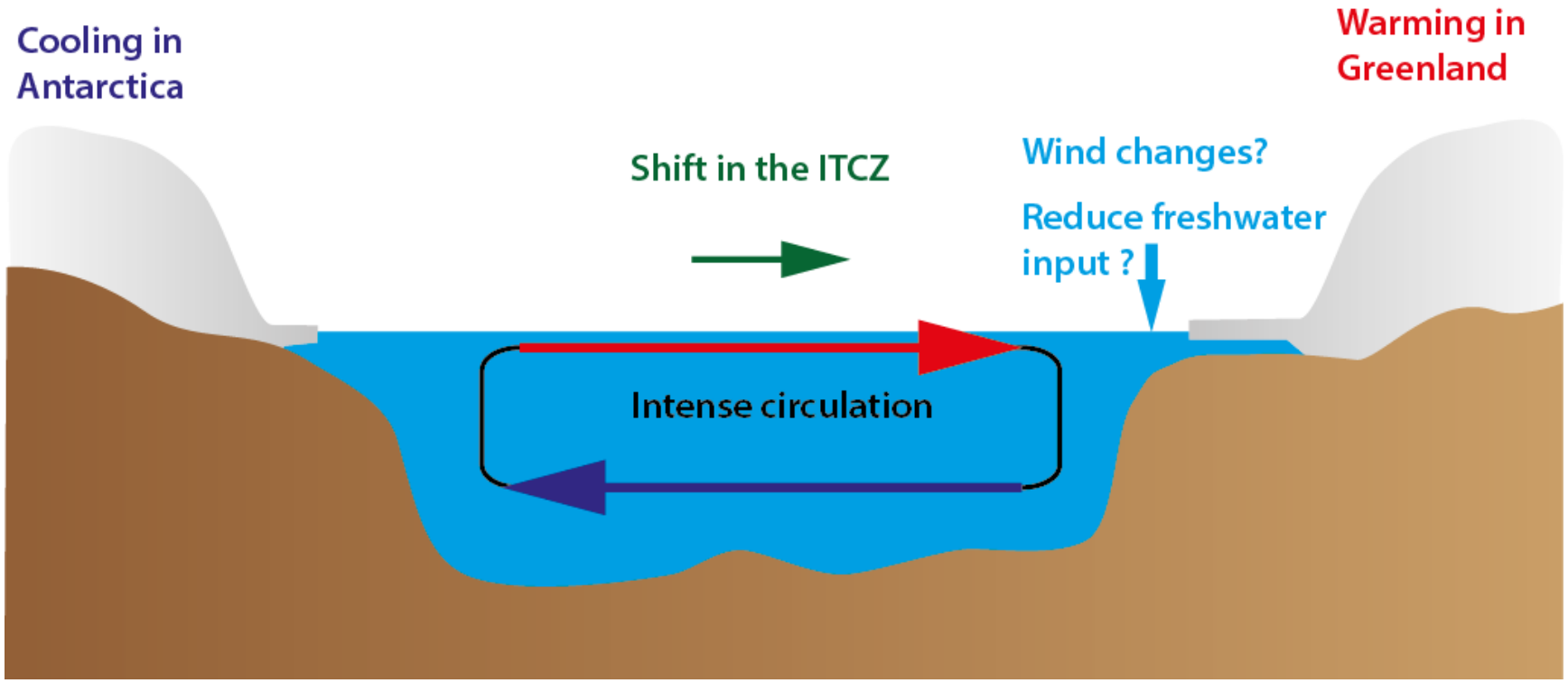

Schematic representation of the processes potentially occurring during Dansgaard-Oeschger events.

The last deglaciation

The increase in CO_2 concentration appears synchronous with the temperature rise in Antarctica.

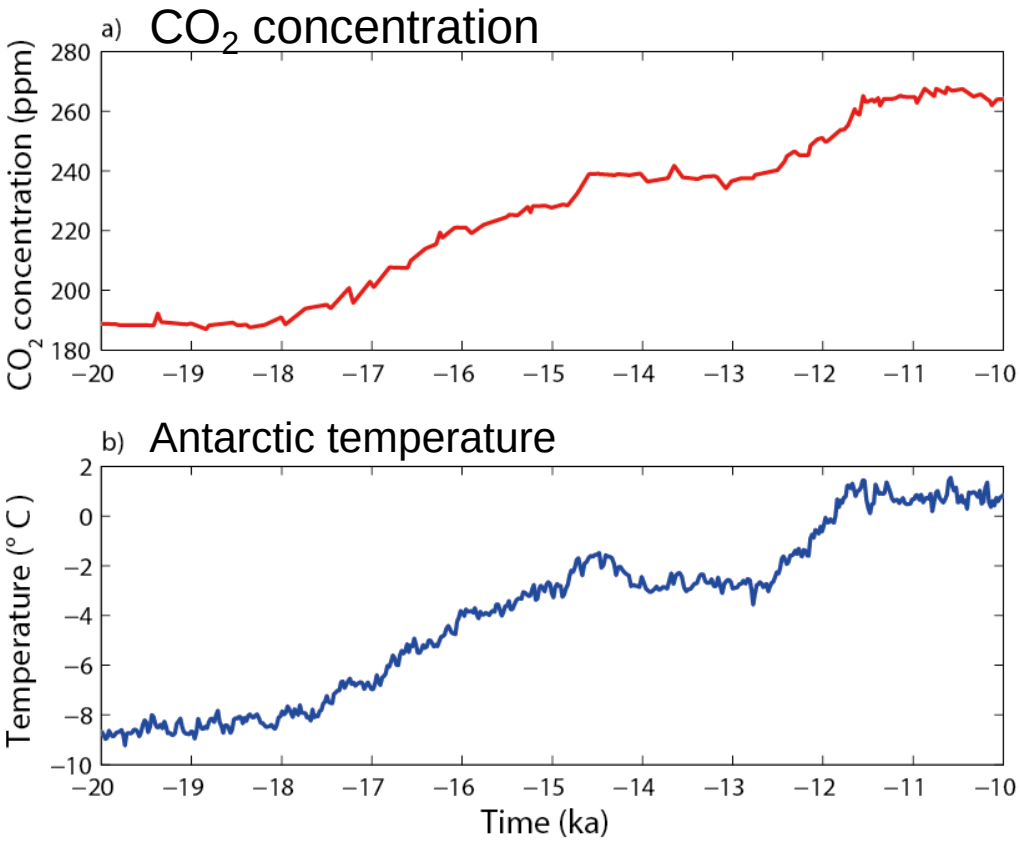

Times series of CO_2 concentration measured in the EDC ice core and Antarctic temperature estimated from a composite of five Antarctic ice cores records during the deglaciation. Data from Parrenin et al. (2013).

The last deglaciation

The deglaciation is also characterized by millennial-scale variability.

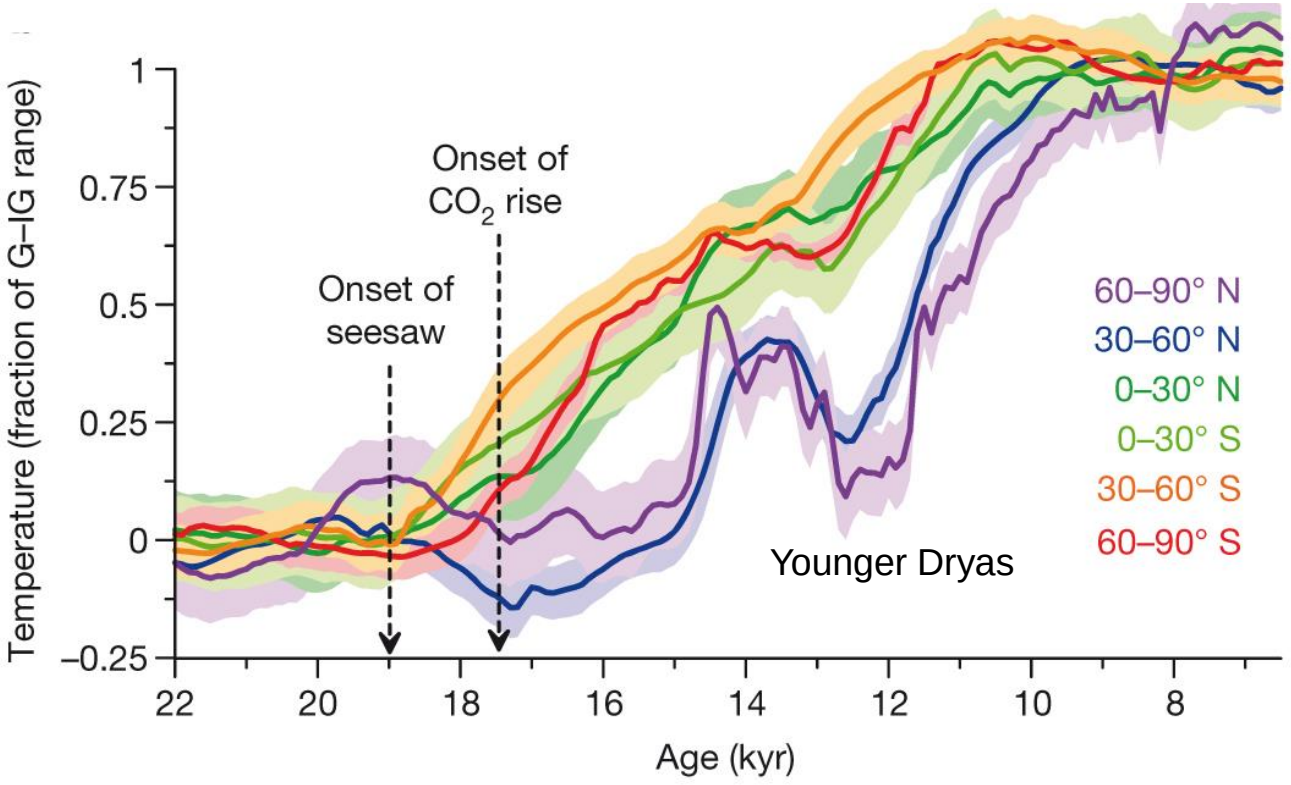

Time series of temperature averaged over different latitudes bands reconstructed from a compilation of various proxies. Figure from Shakun et al. (2012).

The current interglacial –The Holocene

The maximum of summer insolation at high latitudes over the Holocene was reached at the beginning of the interglacial.

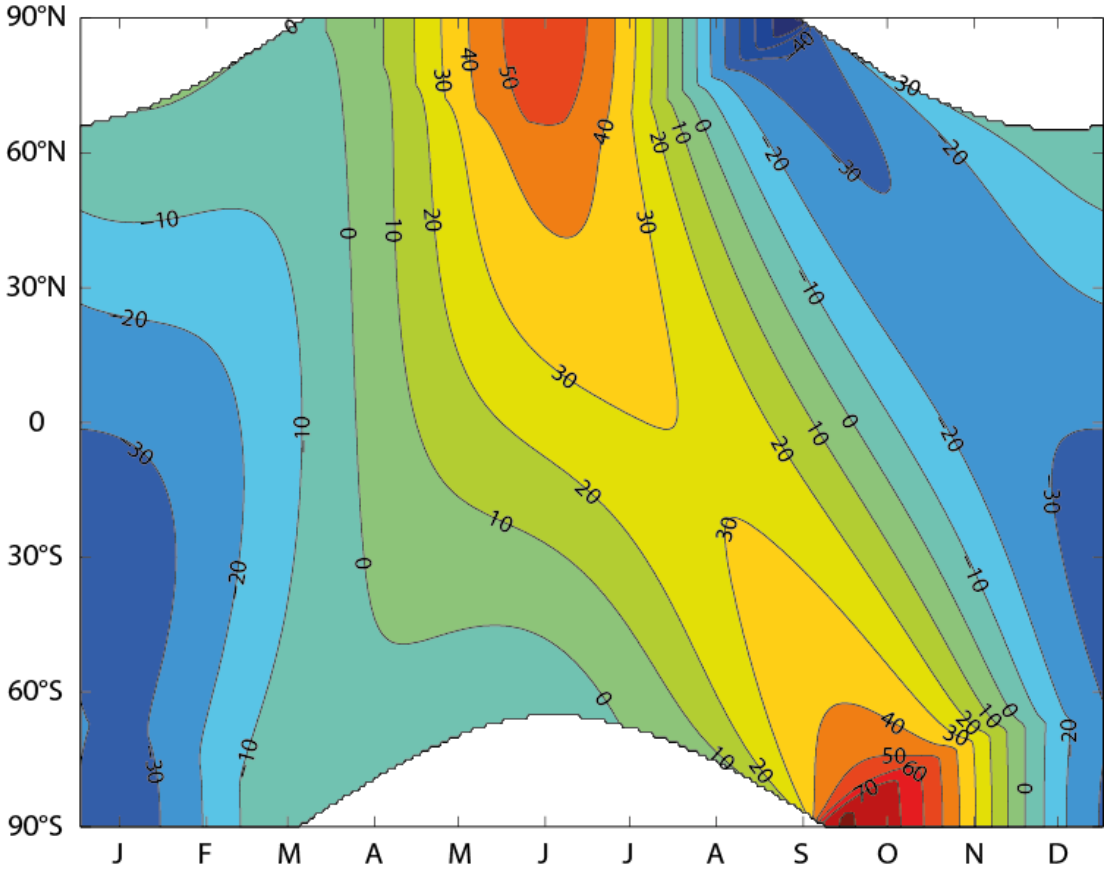

Deviations from present-day values at 10ka BP of the daily insolation for calendar months (in Wm^{-2}). Data from Berger (1978). Figure from Marie-France Loutre.

The current interglacial –The Holocene

The Holocene Thermal Optimum is found between 9 and 6 ka BP in the Northern Hemisphere.

Northern Hemisphere summer monsoon was stronger in the early and mid-Holocene.

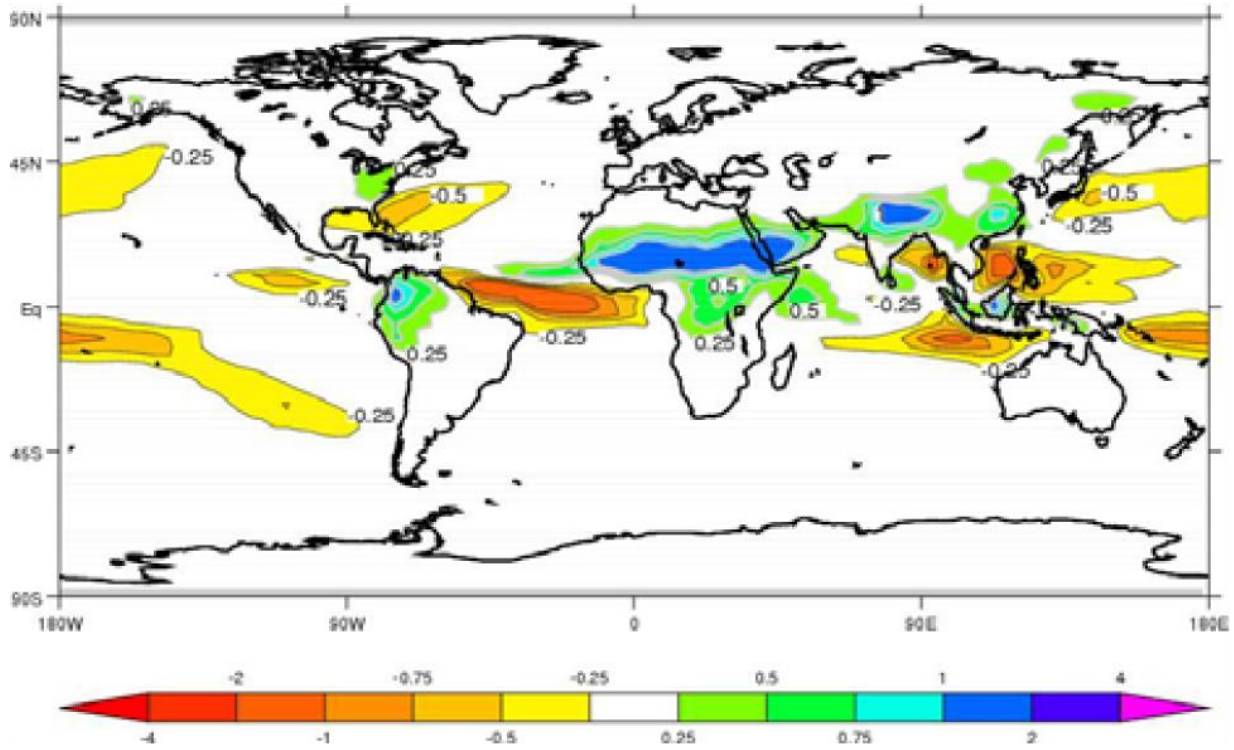

Difference of precipitation (mm/d) between Mid-Holocene (6000 yr BP) and preindustrial conditions for the ensemble mean of PMIP2 simulations. Figure from Braconnot et al. (2007).

The past 2000 years

The global mean temperature shows relatively mild conditions between 950 and 1250 AD and cold conditions between 1450 and 1850 AD.

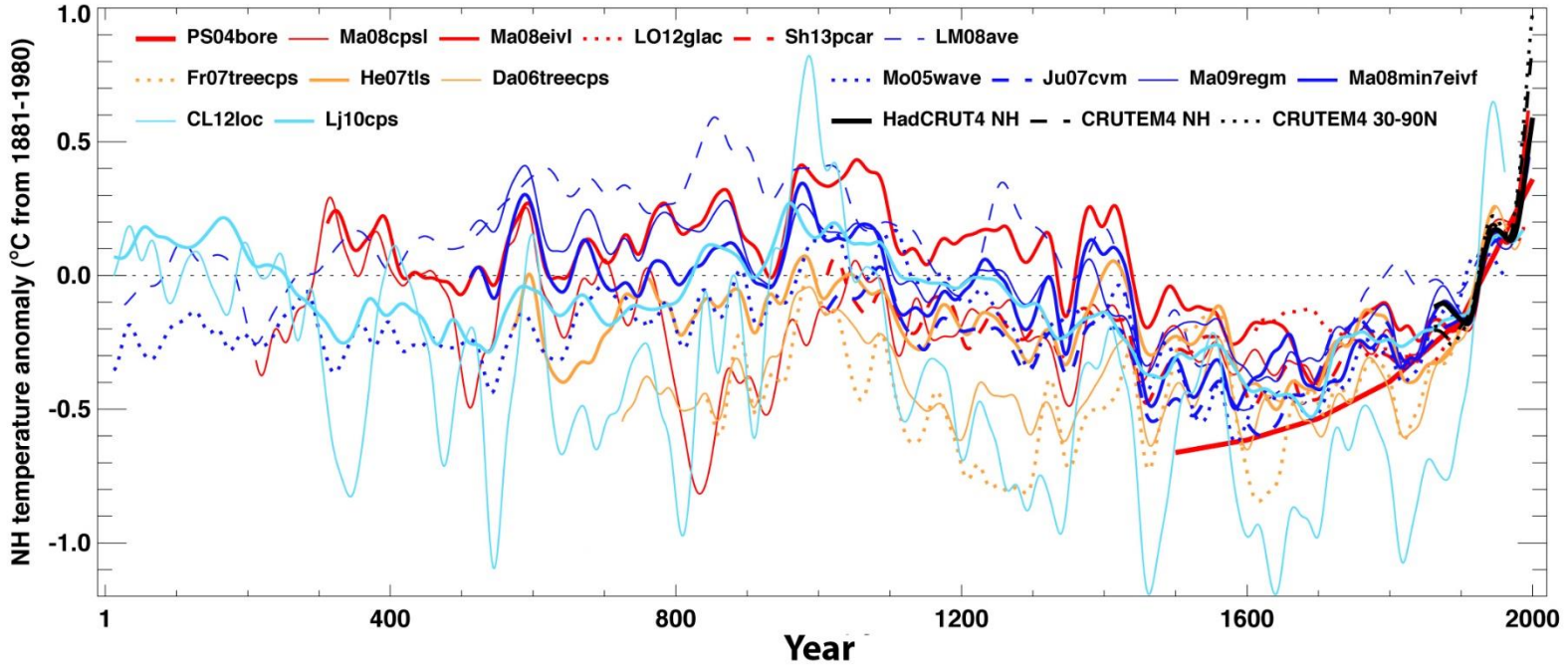

Reconstructions of Northern Hemisphere temperatures during the last 2000 years. Figure from Masson-Delmotte et al. (2013).

The last 30 years were likely the warmest 30-year period of the last 1400 years in the Northern Hemisphere

The past 2000 years

When driven by natural and anthropogenic forcings, model are able to reproduce the observed changes.

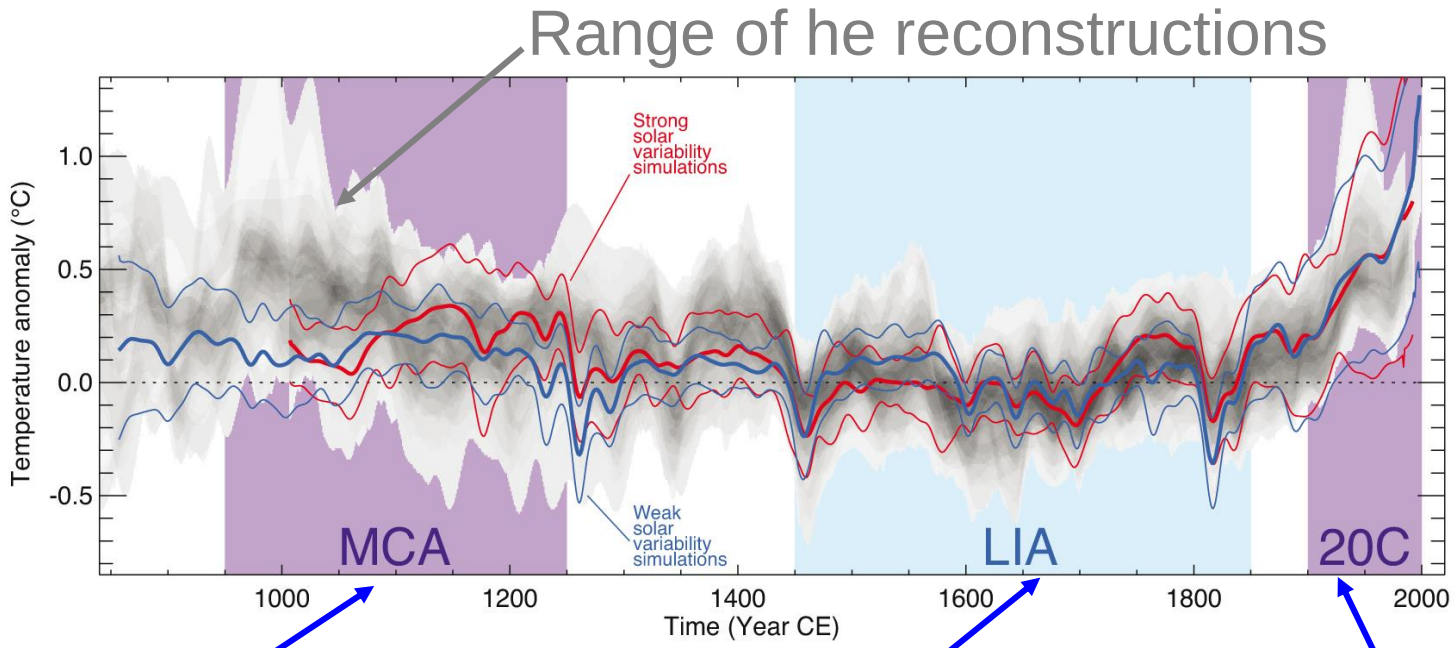

Medieval Climate Anomaly

Little Ice Age

20th century

Comparison of simulated and reconstructed changes over past millennium in the Northern Hemisphere. Figure from Masson-Delmotte et al. (2013).

The past 2000 years

Some characteristics are common, but the warm and cold periods are not synchronous between the different regions.

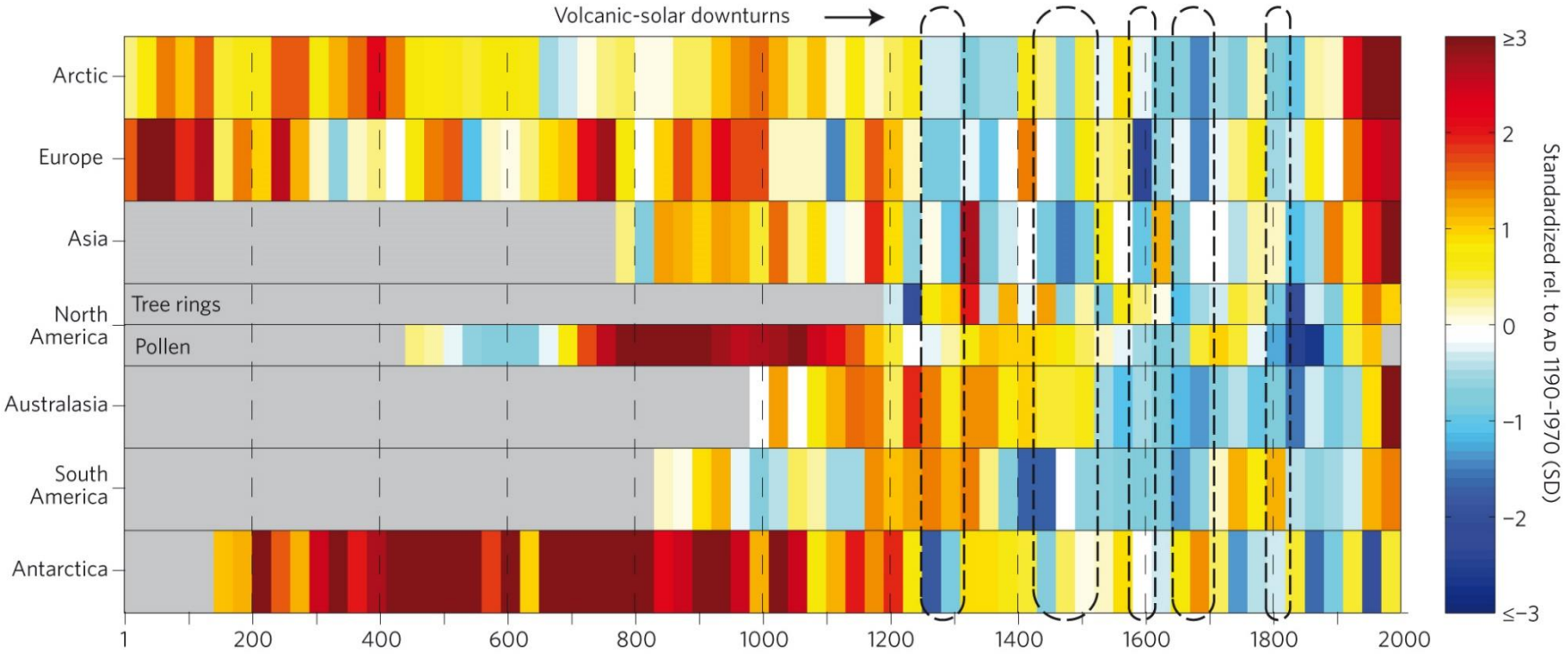

Temperature reconstructions for seven continental-scale regions. Figure from PAGES2K (2013).

The past 2000 years

The internal variability is responsible of some of the warm and cold periods in the different regions.

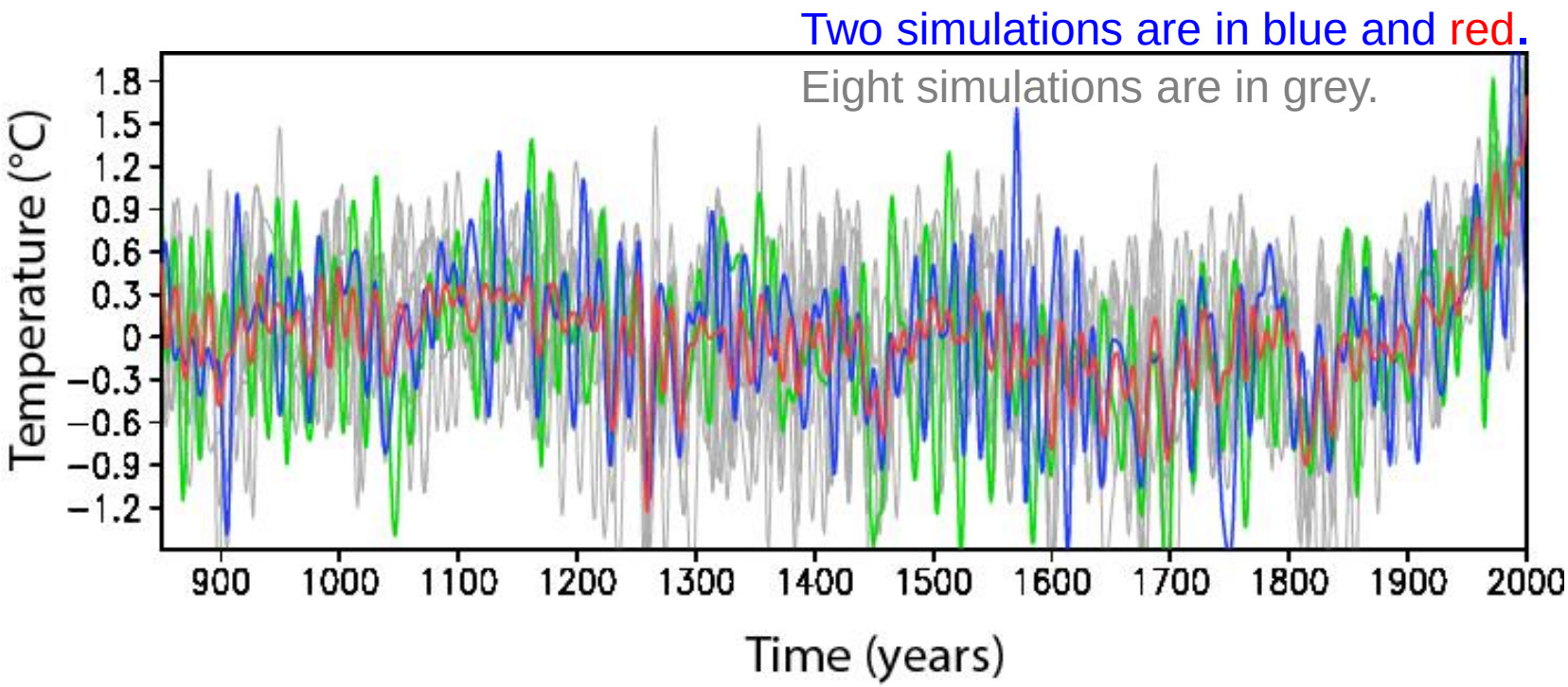

Surface temperature anomaly (°C) in the Arctic over the last millennium in an ensemble of 10 simulations using the same model driven by the same natural and anthropogenic forcings. A decadal smoothing has been applied to the series. Data from Crespin et al. (2013).

The last century

The linear trend of global mean temperature over the years 1901-2012 gives an increase of 0.89°C over that period.

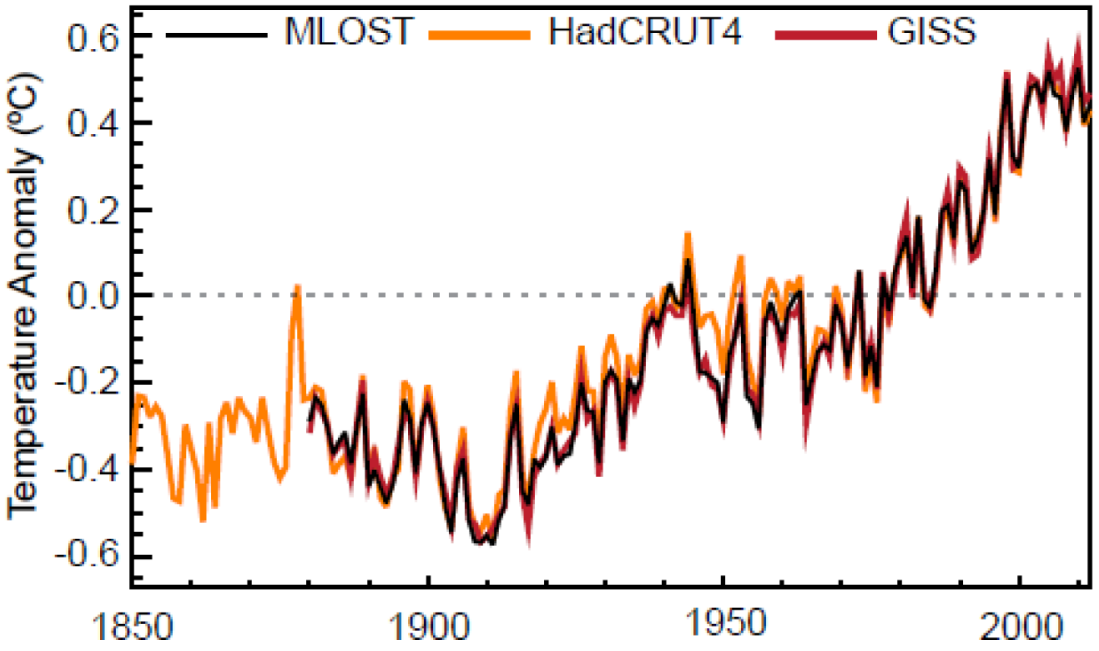

Global mean annual surface temperature (°C) from 1850 to 2012 relative to the 1961 to 1990 mean, from 3 different datasets. Figure from Hartmann et al. (2014).

The last century

The warming is seen in nearly all the regions with generally a slower warming over ocean than over land.

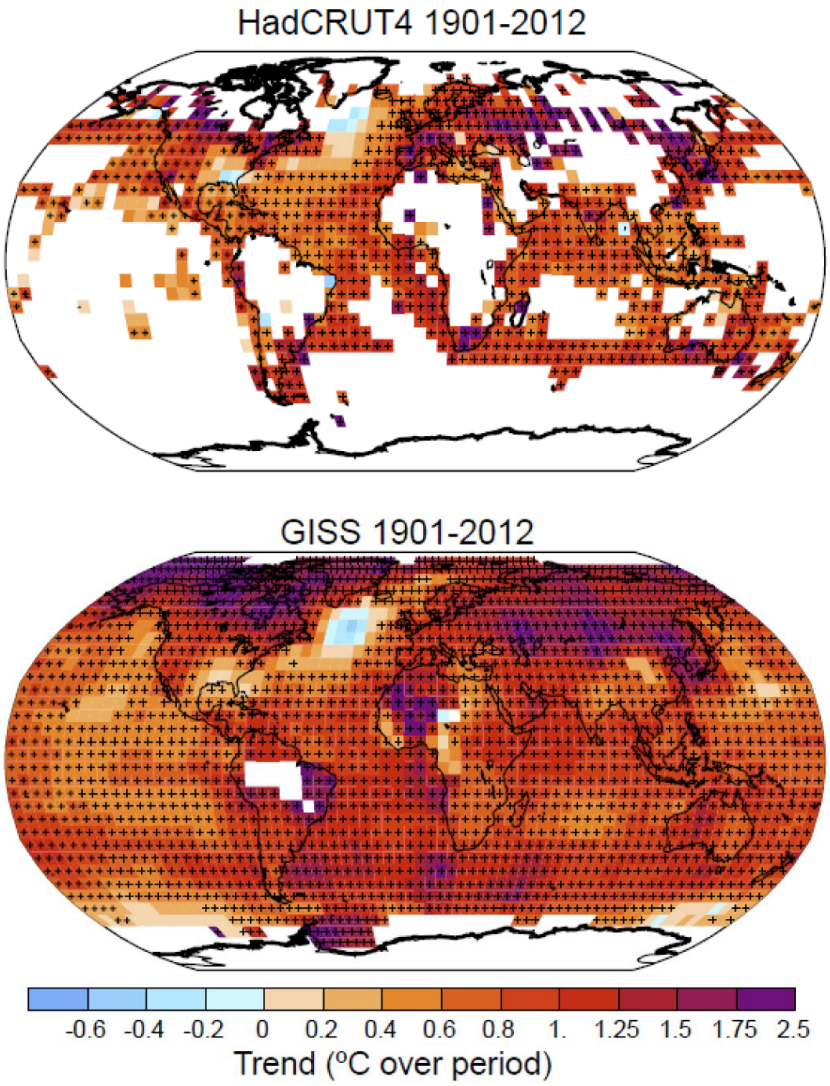

Linear trend of annual temperatures between 1901 and 2012 in HadCRUT4 and GISS datasets (°C over the period). Figure from Hartmann et al. (2014).

Detection and attribution of recent climate changes

The anthropic origin of the rise in atmospheric CO_2 concentration since the 19th century is unequivocal.

The part of the recent temperature changes compatible with the natural variability can be estimated using various techniques.

Detection and attribution of recent climate changes

Simulations using various combinations of forcings can be compared to observations.

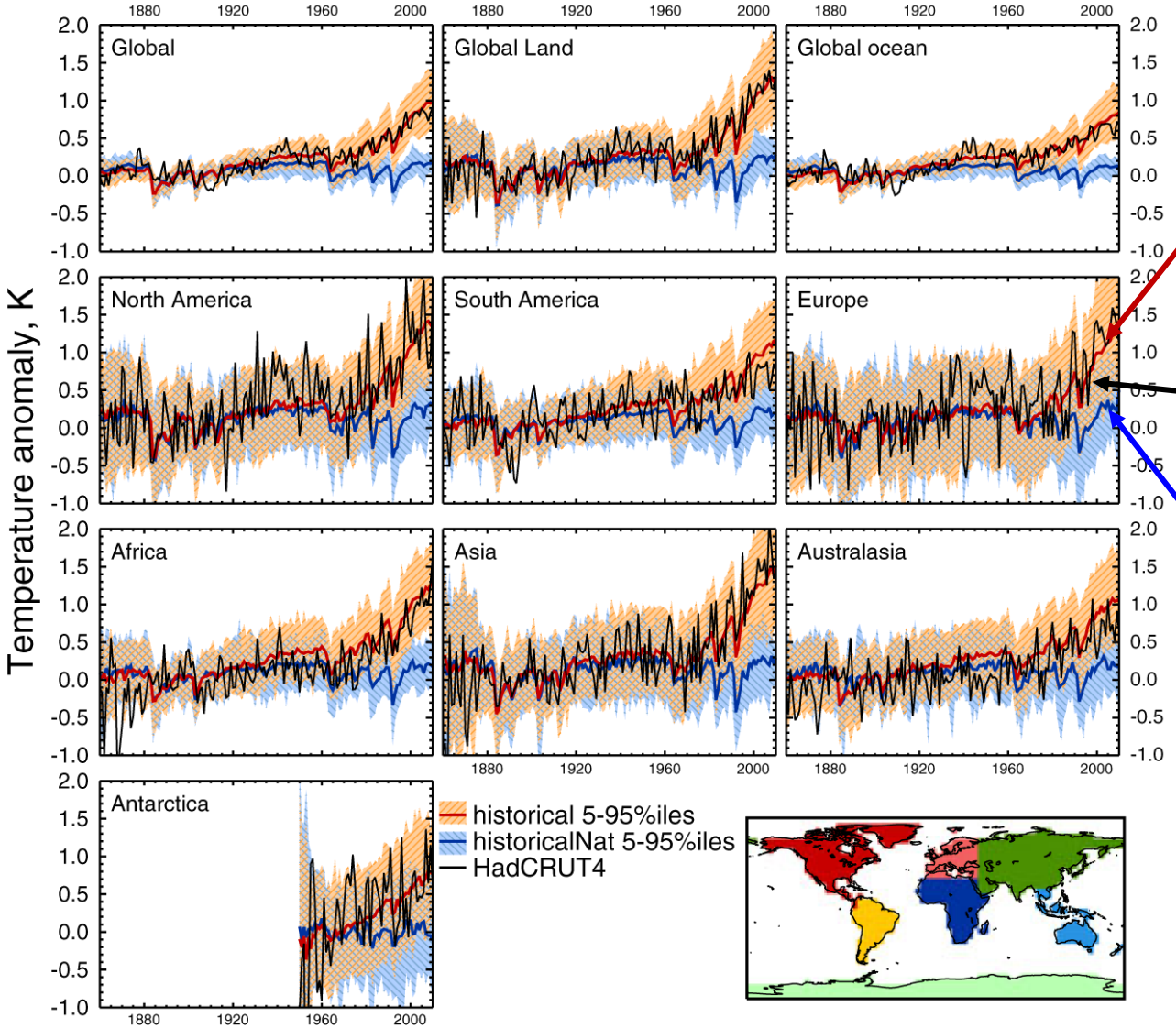

Models with natural and anthropogenic forcings

Observations

Models with natural forcings only

Figure from Jones et al. (2013)

Detection and attribution of recent climate changes

Observations are not compatible with the hypothesis stating that the changes in climate observed recently are in the range of natural variability on decadal to centennial timescales.

Observations are compatible with the hypothesis that anthropogenic forcing is needed to explain the recent temperature changes.

Detection and attribution of recent climate changes

Detection and attribution methods represent the observed changes as the sum of the response to different forcings and internal variability.

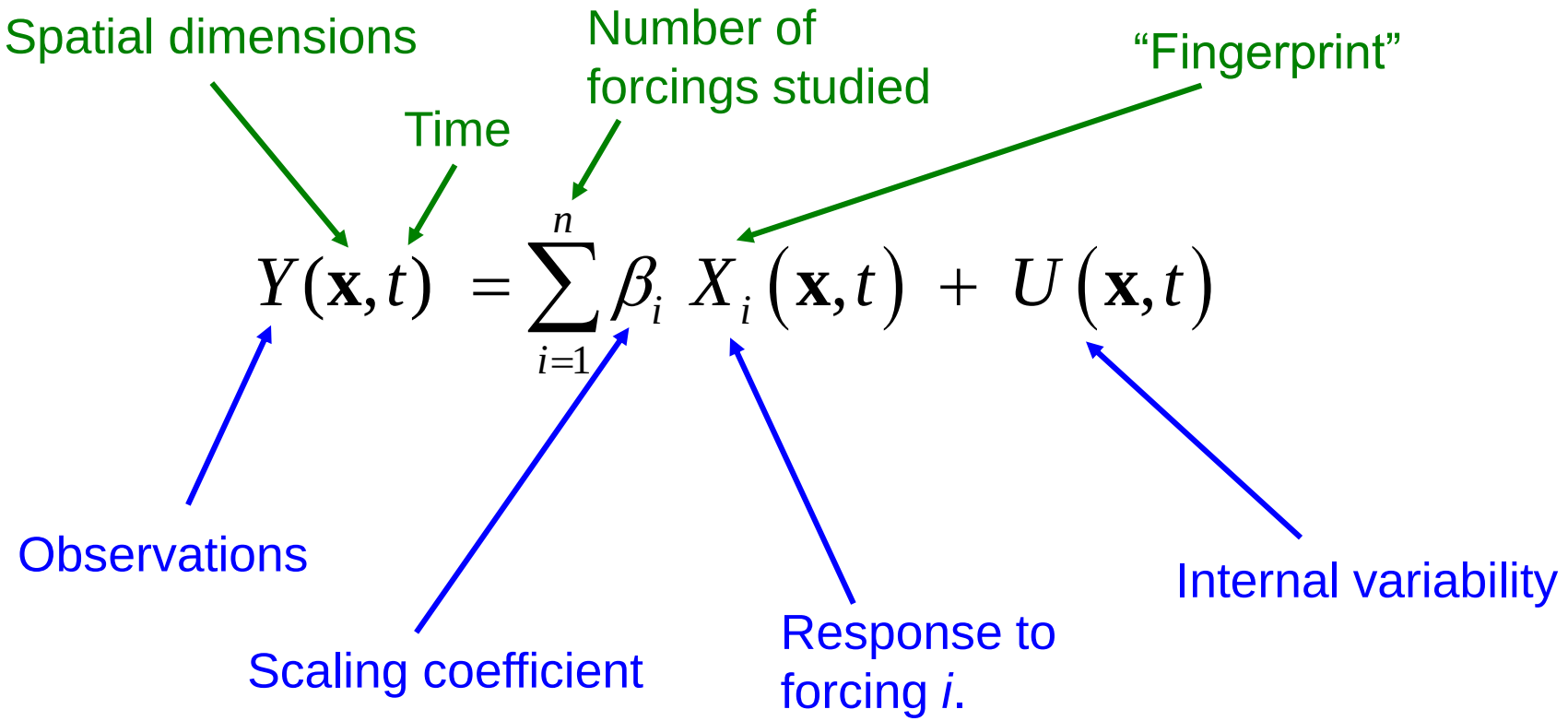

Detection and attribution of recent climate changes

Example: simple, idealised situation, considering an observed time series T(t)

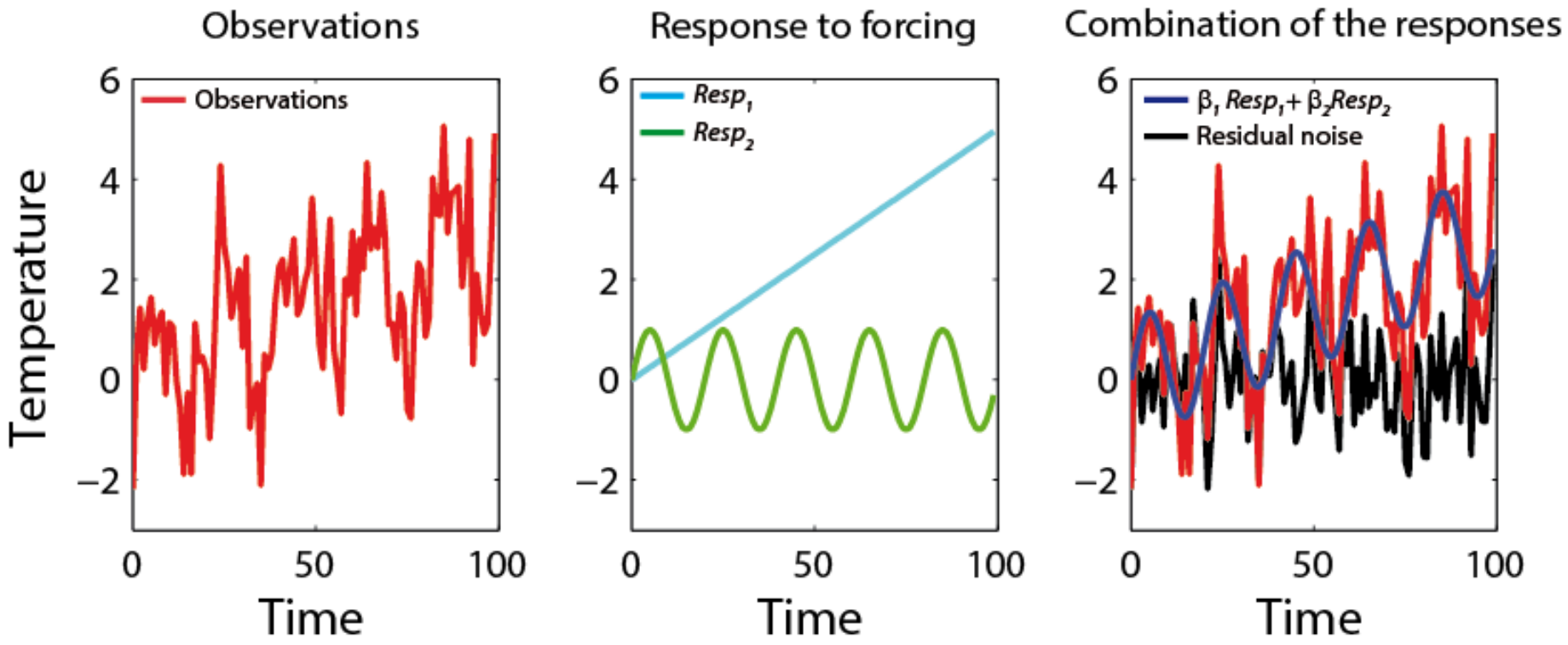

Simple illustration of the detection and attribution method. The observed time series $T(t) = \beta_1 \, Resp_1(t) + \beta_2 \, Resp_2(t)+u(t)$. In the chosen example, the coefficient of the linear combination are $\beta_1=0.6$ and $\beta_2=1.2$.

Detection and attribution of recent climate changes

The contribution of the increase in greenhouse gas concentrations in the atmosphere in the recent warming can be clearly detected.

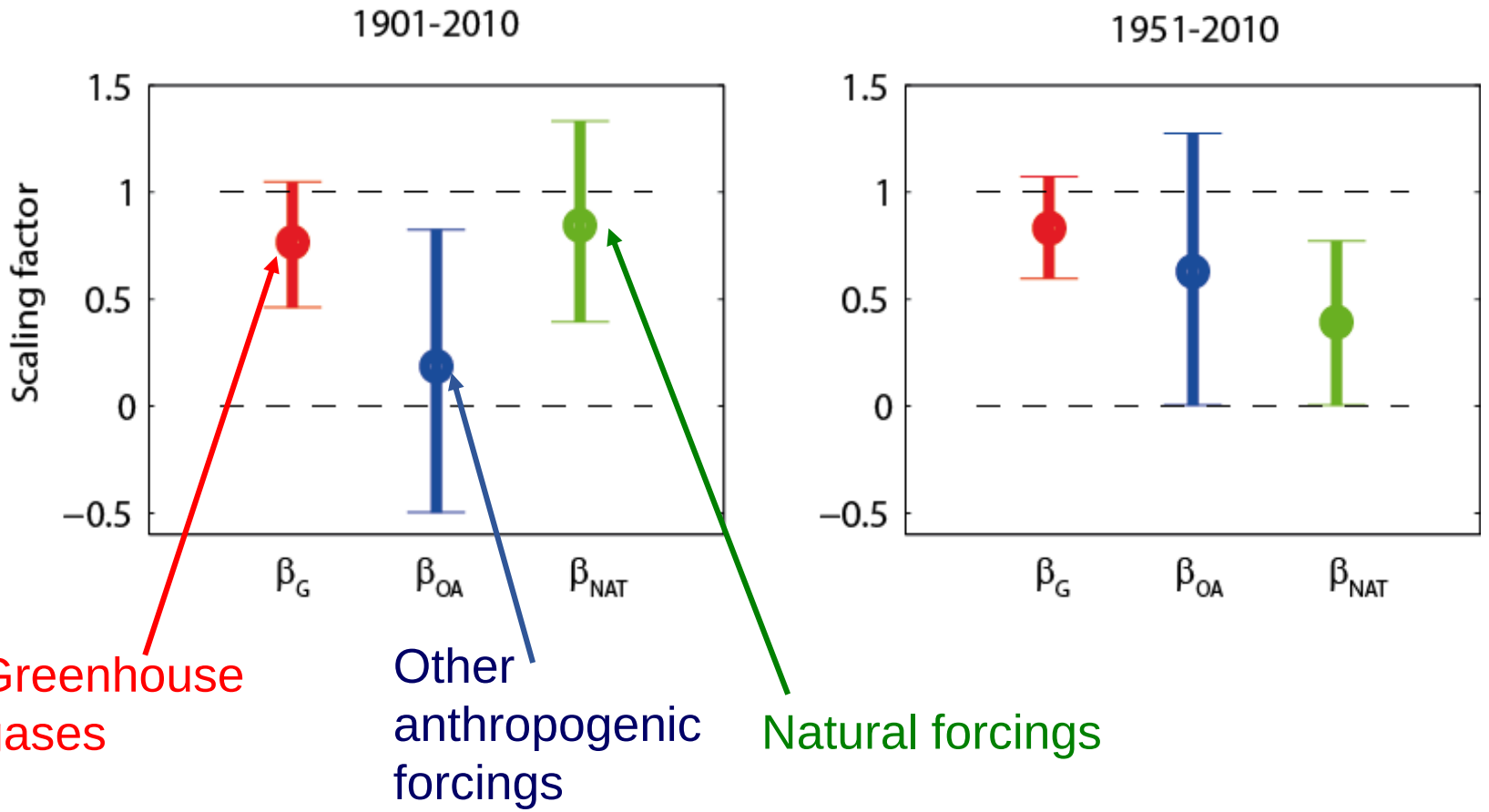

Scaling coefficient in a detection and attribution study. Data from Jones et al. (2013).